Transcriptional dynamics of colorectal cancer risk associated variation at 11q23.1 are correlated with tuft cell abundance and marker expression *in silico*

Bradley T. Harris[1], Vidya Rajasekaran[1], James P. Blackmur[1,2], Alan O'Callaghan[2], Kevin Donnelly[1,2], Maria Timofeeva[1,3], Peter G. Vaughan-Shaw[1,2], Farhat V. N. Din[1], Malcolm G. Dunlop[1,2] and Susan M. Farrington[1,*]

[1] Cancer Research UK Edinburgh Centre, Institute of Genetics and Cancer, University of Edinburgh, United Kingdom

[2] MRC Human Genetics Unit, Institute of Genetics and Cancer, University of Edinburgh, Edinburgh, United Kingdom

[3] Department of Public Health, D-IAS, Danish Institute for Advanced Study, University of Southern Denmark, Odense, Denmark

* Corresponding author: susan.farrington@ed.ac.uk

Keywords: colorectal cancer; risk; eQTL (expression quantitative trait loci); scRNAseq (single cell RNA sequencing); WGCNA (weighted gene co-expression network analysis); linear modelling

Abstract

Colorectal cancer (CRC) is characterised by heritable risk that is not well understood. Heritable, genetic variation at 11q23.1 is associated with increased colorectal cancer (CRC) risk, demonstrating eQTL effects on 3 cis- and 23 trans-eQTL targets. We sought to determine the relationship between 11q23.1 cis- and trans-eQTL target expression and test for potential cell-specificity. scRNAseq from 32,361 healthy colonic epithelial cells was aggregated and subject to weighted gene co-expression network analysis (WGCNA). One module (blue) included 19 trans-eQTL targets and was correlated with *C11orf53* expression only. Following unsupervised clustering of single cells, the expression of 19 trans-eQTL targets was greatest and most variable in cluster number 11, which transcriptionally resembled tuft cells. 14 trans-eQTL targets were found to demarcate this cluster, 11 of which were corroborated in a second dataset. Intra-cluster WGCNA and module preservation analysis then identified twelve 11q23.1 trans-eQTL targets to comprise a network that was specific to cluster 11. Finally, linear modelling and differential abundance testing showed 11q23.1 trans-eQTL target

35 expression was predictive of cluster 11 abundance. Our findings suggest 11q23.1 trans-eQTL
36 targets comprise a *C11orf53*-related network that is likely tuft cell-specific and reduced
37 expression of these genes correlates with reduced tuft cell abundance *in silico.*
38
39 **Introduction**
40
41 Colorectal cancer (CRC) is the fourth most common cancer type UK and worldwide (Cancer
42 Research UK, 2017; Rawla et al., 2019). Approximately 40% of CRC risk is attributable to
43 heritable genetic variation (Graff et al., 2017), with rare, highly penetrant mutations
44 responsible for a small fraction of overall risk (Jasperson et al., 2010; Sud et al., 2017).
45 Genome wide association studies (GWAS) have identified 129 common genetic variants
46 associated with CRC risk (Huyghe et al., 2019; Law et al., 2019). Several common CRC
47 genetic risk variants are associated with heritable changes in the expression levels of genes
48 in colonic mucosa, known as expression quantitative trait loci (eQTLs) (Closa et al., 2014;
49 Hulur et al., 2015; Loo et al., 2017; Vaughan-Shaw et al., 2021).
50
51 Genetic variation at 11q23.1 is associated with increased CRC risk (Tenesa, Farrington et al.,
52 2008). However, the large number of variants in high linkage disequilibrium at 11q23.1 makes
53 identifying the causal variant, a key step to identifying the mechanism of gene dysregulation,
54 difficult. Studies have shown that CRC risk associated variation at several 11q23.1 variants is
55 correlated with the downregulation of three local genes; *C11orf53, COLCA1, COLCA2*
56 (Biancolella et al., 2014; Loo et al., 2017; Smillie, 2015), known as cis-eQTL targets. We have
57 recently shown that variation at rs3087967, a single nucleotide variant in the 3'UTR of
58 *C11orf53*, is significantly correlated with distal CRC risk and a myriad of distant, trans-eQTL
59 targets throughout the colon (Vaughan-Shaw *et al.,* 2021), Additional File 1. Of these, only
60 two have a common, well-described function; *IL17RB* and *TRPM5* are experimentally
61 determined markers of tuft cells - a rare epithelial cell-type (Haber et al., 2017; Kaske et al.,
62 2007). The function of several other trans-eQTL targets is currently unknown and their exact
63 relevance to both 11q23.1 cis-eQTL target expression and CRC risk is not characterised.
64
65 Current methods of eQTL detection, while widely used, exhibit some key limitations. eQTLs
66 are frequently identified by linear models of bulk RNA-seq/microarray transcriptome analysis
67 of healthy tissue (Michaelson et al., 2009; Richards et al., 2012; Stranger et al., 2007). These
68 methods often treat both gene expression and single-nucleotide polymorphisms as
69 independent, linear entities: assumptions which over-simplify the complex relationships

70 governing gene expression dynamics and limit results to additive gene-dosage related findings.
71 In addition, eQTL analyses require performance of an extremely large number of independent
72 tests to be conducted, limiting its sensitivity. Correlation-based methods of gene expression
73 analysis, such as weighted gene co-expression network analysis (WGCNA, Langfelder &
74 Horvath, 2008), circumvent this problem by agnostically identifying correlations between
75 individual genes, and entire, non-overlapping gene modules, with binarized categorical or
76 quantitative traits. Modules of correlated genes may themselves be correlated with sample
77 phenotypes. In addition, WGCNA also does not require a hard thresholding of correlations, a
78 major advantage over other correlation-based methods that rely on arbitrary cut offs. We have
79 recently shown that WGCNA can be efficacious at identifying genes driving transcriptional
80 dynamic changes in the colorectum of patients treated with Vitamin D (Blackmur et al., 2022),
81 even in the absence of statistically significant changes in differential expression analysis.
82 Moreover, as CRC risk-associated eQTL targets are identified by bulk expression methods,
83 findings are inherently limited in their potential to detect cell-specific changes, particularly in
84 rare cell-types; expression changes within which may be masked due to low relative
85 abundance.
86
87 We hypothesised that the expression of 11q23.1 trans-eQTL targets may be correlated with
88 only a single cis-eQTL target, a relationship which may in turn be specific to a single epithelial
89 cell-type in the colon. We utilised WGCNA across and within single-cell RNA sequencing
90 (scRNAseq) clusters to further characterise eQTL target expression relatedness in colonic
91 epithelial cell-types. An overview of the analysis performed in this study is shown in Figure 1.
92
93 **Results**
94
95 ***Understanding cis-eQTL specificity of 11q23.1 trans-eQTL effects***
96
97 To test potential colonic epithelial cell-specificity of 11q23.1 eQTL effects, we sought to
98 analyse the expression of target genes within colonic epithelial cell-types. To this end, we
99 obtained scRNAseq from 32,361 healthy human colonic mucosa epithelial cells from eleven
100 individuals (Smillie et al., 2019). To first assess the validity of this dataset in studying 11q23.1
101 variation-related expression dynamics, we devised a method of pseudo-bulking the
102 expression from all cells in this dataset, aggregating the expression of every gene across all
103 cells from each sample (see Figure 1 and Methods). Pseudo-bulked expression from 11q23.1
104 nominally significant trans-eQTL targets, present in the scRNAseq dataset ($p<0.01$, $n=273$),

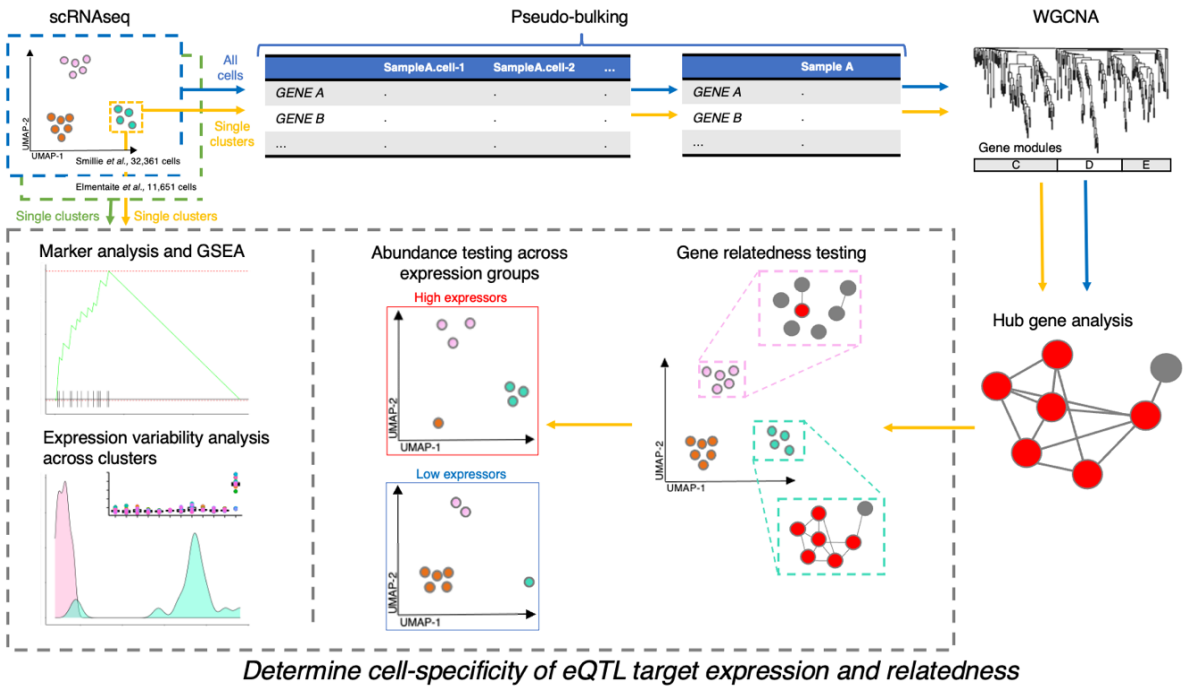

Figure 1. Overview of study design and analysis. This study makes use of two single cell RNA sequencing (scRNAseq) datasets: Smillie *et al.,* (2019) – n=32,261 and Elmentaite *et al.,* (2021) - n=11,651. The analysis performed on each dataset is outlined by arrow colour: blue=all cells from Smillie *et al.,* (2019), yellow=individual clusters from Smillie *et al.,* (2019), green=individual clusters from Elmentaite *et al.,* (2021). WGCNA=Weighted Gene Co-expression Network Analysis, GSEA=Gene Set Enrichment Analysis.

Figure 2A, was then subject to WGCNA (Langfelder & Horvath, 2008). Genes were agnostically grouped into modules of correlated expression, and the correlation between the eigenvector (first principal component) of each module with sample traits and pseudo-bulked cis-eQTL target gene expression was calculated, Figure 2B. The blue module, comprising 77 genes, was found to correlate with *C11orf53* expression (cor=0.81, FDR=2e-04), but none of the sample traits, *COLCA1* or *COLCA2* expression. The blue gene module includes 17 of the 20 significant 11q23.1 trans-eQTL targets that passed gene filtration quality control (FDR<0.05, Vaughan-Shaw *et al.,* 2021); *ALOX5, SH2D6, TRPM5, BMX, PSTPIP2, GNG13, IL17RB, HTR3E, PTGS1, SH2D7, OGDHL, MATK, PLCG2, LRMP, PIK3CG, HTR3C* and *CAMP*, thus indicating the genes comprising this module are specifically related to the expression of *C11orf53,* Supplementary Table 2.

To assess the contribution of 11q23.1 genes to the correlation of the blue module with *C11orf53,* we performed gene set enrichment analysis of the 11q23.1 trans-eQTL target genes (FDR<0.05) against the genes in the blue module, ranked by their module membership - a measure of their relatedness to all other genes in the module (Langfelder & Horvath, 2008). We found the genes in this module are highly enriched for 11q23.1 trans-eQTL targets,

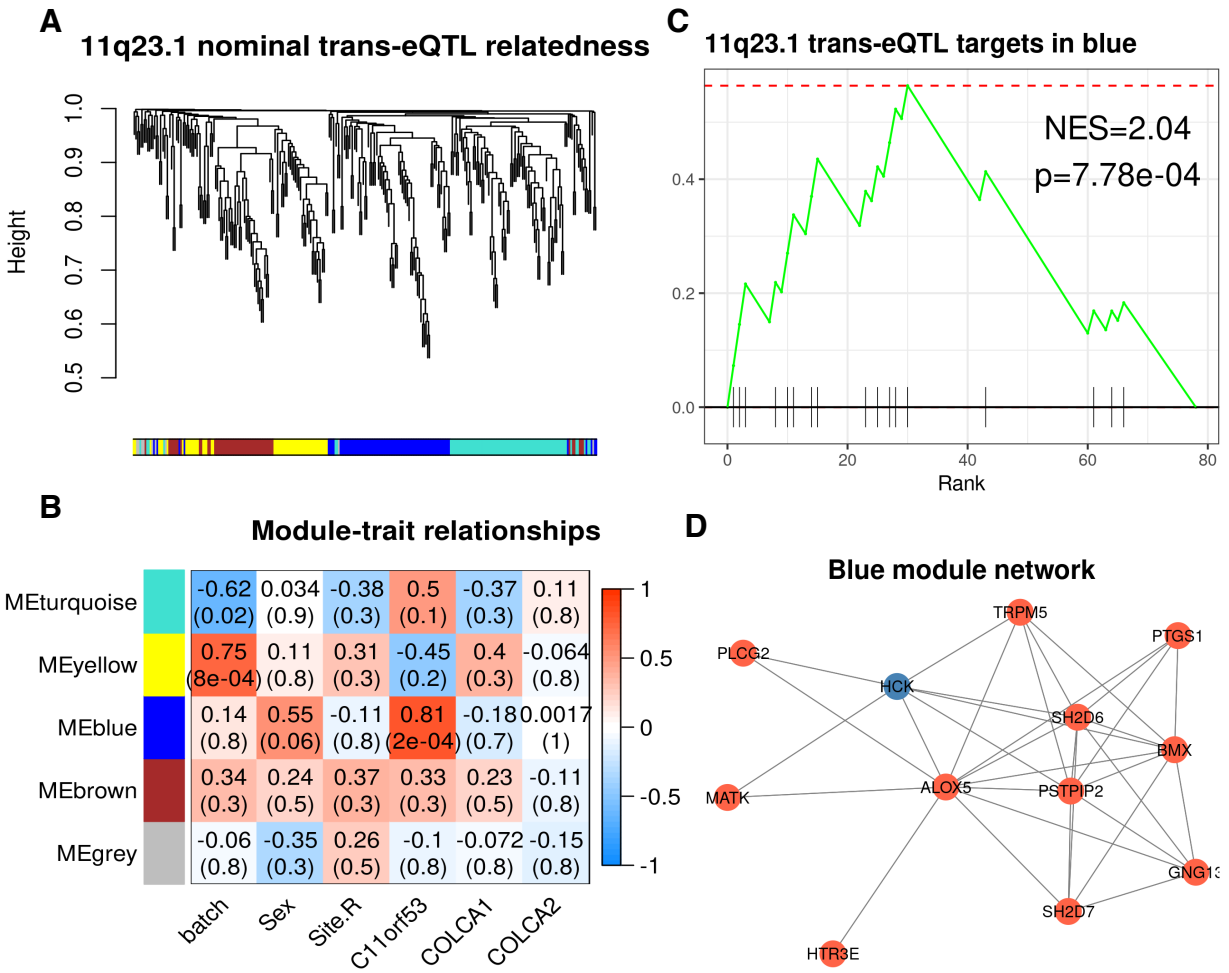

Figure 2. 11q23.1 trans-eQTL targets are correlated with the expression of *C11orf53,* but not *COLCA1* or *COLCA2* in pseudo-bulked scRNASeq. (A) Hierachical clustering of complete distances between pairwise correlations of 11q23.1 nominal trans-eQTL targets pseudo-bulked expression (p<0.01, n=273) in 32,361 healthy colonic epithelial scRNAseq. (B) Weighted Gene Co-expression Network Analysis (WGCNA) identified module trait relationships. Pearson correlations shown above Benjamini-Hochberg corrected p-values in brackets. (C) Gene Set Enrichment Analysis (GSEA) of 11q23.1 trans-eQTL targets (FDR<0.05) in blue module genes, ranked by their module membership. (D) Kamadakawai network of Blue module relatedness (adjacency > 0.3). Red nodes indicate FDR<0.05 trans-eQTL target of 11q23.1.

normalised enrichment score (NES) = 2.04, p=7.78e-04, Figure 2C. In addition, 11 trans-eQTL targets comprised the 12 genes with the greatest adjacency in the blue module (adjacency > 0.3), Figure 2D. We also find that module membership is highly correlated with gene significance for *C11orf53* in the blue module, reinforcing the overall correlation of the network with *C11orf53* expression (Supplementary Figure 1). Together, this replicates the trans-eQTL target expression relatedness previously described (Vaughan-Shaw et al., 2021) and indicates that the expression of the majority of significant 11q23.1 trans-eQTL target genes is correlated with *C11orf53* specifically in this dataset.

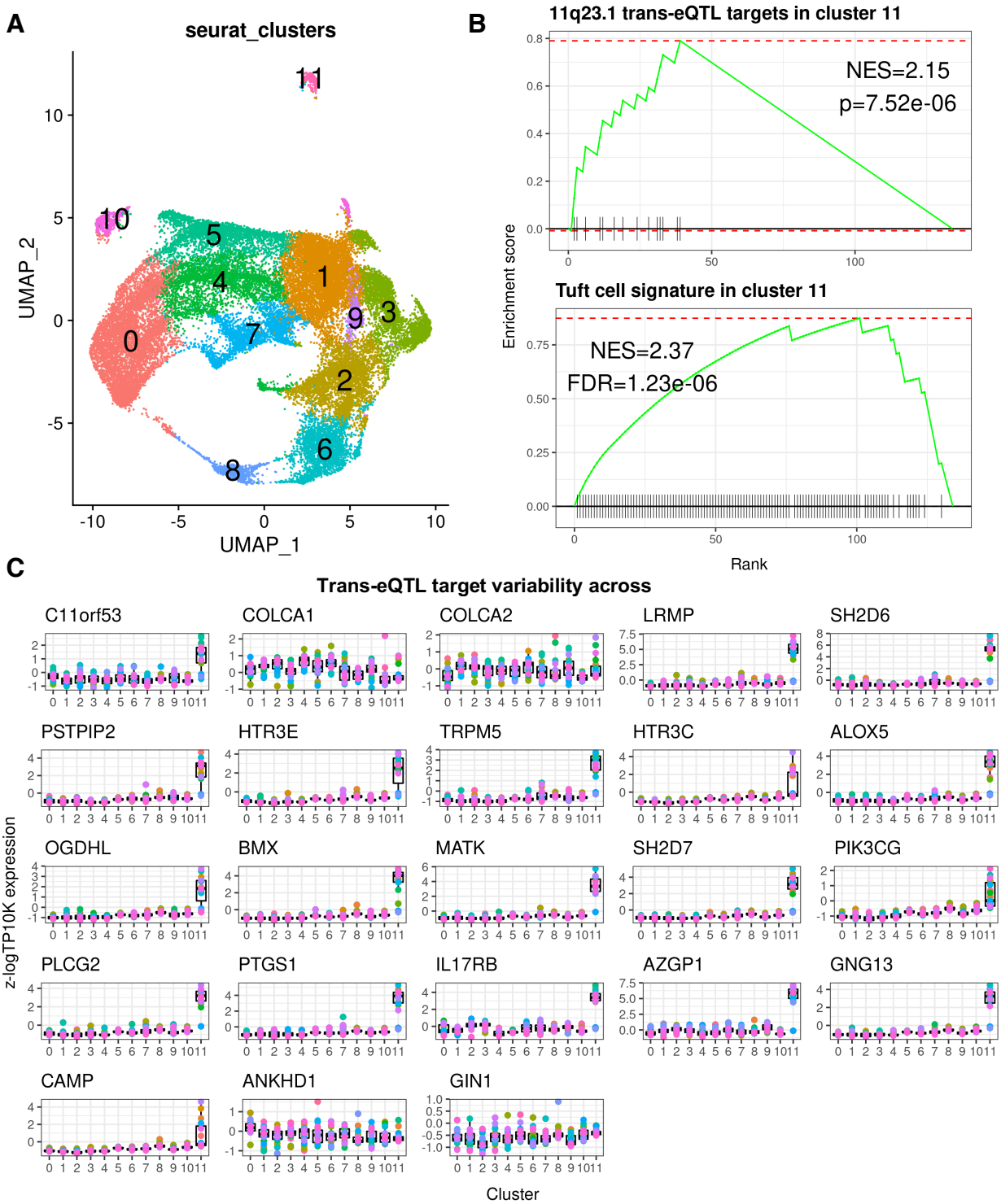

Figure 3. 11q23.1 trans-eQTL expression demarcates tuft-like cell cluster. (A) UMAP of 32,361 epithelial scRNASeq, coloured by cell cluster - identified using Seurat (Hao et al., 2021). (B) Upper: GSEA of 11q23.1 trans-eQTL targets (Vaughan-Shaw *et al.,* 2021; FDR<0.05) in cluster 11 markers. Lower: GSEA of putative colonic tuft cell signature (Smillie *et al.,* 2019) in cluster 11 markers. P=P value, FDR=False Discovery Rate (C) Relative, pseudo-bulked expression (log transcripts per 10,000) of 11q23.1 trans-eQTL targets (FDR<0.05) across clusters.

131 ***Analysing cell-specificity of 11q23.1 eQTL target expression***

132

133 To test the potential for cell-specific expression of 11q23.1 eQTL targets in this dataset, we
134 performed dimensionality reduction and clustering of the single cells, identifying a total of 12
135 transcriptionally distinct cell-clusters, named '0'-'11', Figure 3A. We then calculated the
136 markers of each cluster and found the markers of cluster 11, comprising 318 cells, includes
137 fourteen 11q23.1 trans-eQTL targets (FDR<0.05), Table 1 (full list of cluster 11 marker genes
138 available in Additional File 2). In addition, cluster 11 markers are significantly enriched for
139 11q23.1 trans-eQTL targets (NES=2.15, p=7.52e-06), Figure 3B. Cluster 11 was found to
140 transcriptionally resemble the Smillie *et al.,* tuft cell cluster, by enrichment of each cluster's
141 markers with the authors' putative markers (NES=2.37, FDR=1.23e-06, see Methods).
142 Together, this indicates cluster 11 is transcriptionally defined by the expression of 11q23.1
143 trans-eQTL targets, several of which are themselves putative tuft cell markers.

144

145 Because the expression of 11q23.1 trans-eQTL targets is reduced in individuals with the CRC
146 risk-associated genotype at 11q23.1 (Vaughan-Shaw et al., 2021), we wanted to assess the
147 variability in the expression of these genes within each cluster. We pseudo-bulked the
148 expression of all cells from each sample, within clusters, and analysed 11q23.1 trans-eQTL
149 target expression (Figure 3C). The relative expression level and variability of *C11orf53* and 18
150 of the 11q23.1 trans-eQTL targets is overwhelmingly greatest within cluster 11, indicating the
151 eQTL effect on these genes is exacerbated within this cluster. Notably, the relative variation
152 and expression of cis-eQTL targets *COLCA1* and *COLCA2* and trans-eQTL targets *ANKHD1*
153 and *GIN1,* is not greatest within this cluster, suggesting the eQTL effect on these genes may
154 not be driven by transcriptional dynamics within this cell-type. In addition, we analysed
155 11q23.1 eQTL target variability at the single cell level, Supplementary Figure 2. The variability
156 of *C11orf53* and the same 18 trans-eQTL targets was found to be greatest within cluster 11,
157 replicating the potential exacerbation of the eQTL effect within this cluster and supporting the
158 validity of our pseudo-bulk method. *C11orf53* expression, however, was not found to
159 demarcate cluster 11 by marker identification analysis (see Methods), data not shown.

160

161 To test the robustness of tuft cell-like mapping of 11q23.1 trans-eQTL target expression and
162 variability, we replicated this analysis in an independent dataset of 11,651 healthy adult
163 colonic epithelial cells from 3 individuals (Elmentaite et al., 2021), Supplementary Figure 4A.
164 In this instance, we identified 19 cell-clusters by dimensionality reduction and unsupervised
165 clustering, named '0'-'18'. The markers of cluster 18 were significantly enriched for the

Gene	p_val	avg_log2FC	pct.1	pct.2	p_val_adj
AZGP1	1.00E-279	2.5735445	0.72	0.029	1.00E-279
SH2D6	1.00E-279	2.43533298	0.736	0.007	1.00E-279
LRMP	1.00E-279	1.97284472	0.572	0.005	1.00E-279
PTGS1	1.18E-278	1.33766533	0.459	0.003	1.75E-274
IL17RB	1.00E-264	1.04046297	0.412	0.031	1.48E-260
BMX	7.18E-248	1.18575976	0.406	0.002	1.07E-243
ALOX5	8.25E-244	1.09872574	0.409	0.003	1.22E-239
MATK	2.88E-240	1.3710223	0.406	0.003	4.28E-236
SH2D7	2.50E-235	1.20590753	0.393	0.002	3.72E-231
GNG13	2.93E-220	0.98868335	0.362	0.001	4.34E-216
TRPM5	1.32E-214	0.94972732	0.377	0.004	1.96E-210
PLCG2	1.22E-209	0.98215989	0.365	0.002	1.82E-205
PSTPIP2	2.21E-197	0.87613246	0.333	0.004	3.28E-193
HTR3E	4.86E-184	0.8684383	0.308	0.001	7.21E-180

Table 1. 11q23.1 trans-eQTL targets identified as cluster 11 markers. Markers calculated using MAST (McDavid *et al.,* 2020). Avg_log2FC=average log2 fold change between cluster 11 and all other clusters. Pct1=Proportion of gene expression in cluster 11. Pct2=Proportion of expression in non-cluster 11. P_val_adj=FDR-corrected p-value.

166 expression of 11q23.1 trans-eQTL targets (NES=2.50, P=5.52e-09, Supplementary Figure
167 4B), 11 of which were identified as markers of this cluster, Supplementary Table 3. Cluster 18
168 was also enriched for the tuft cell signature (NES=2.41, P=7e-08), replicating our previous
169 finding. The relative variability and expression of the majority of 11q23.1 trans-eQTL targets
170 was also greatest within cluster 18, Supplementary Figure 4C. The expression of 13 trans-
171 eQTL targets was also most variable within cluster 18 when expression was analysed at the
172 single cell level, Supplementary Figure 4. Interestingly, *C11orf53* expression variability was
173 not found to vary greatest within cluster 18 when using expression from single cells.
174
175 ***Understanding 11q23.1 cis- and trans-eQTL relatedness within clusters***
176
177 The demarcation and variability of 11q23.1 trans-eQTL target expression within a tuft-like cell
178 cluster strongly indicates the eQTL effect is derived from altered gene expression in this cell-
179 type specifically. However, it is possible that the gene-gene relatedness of 11q23.1 eQTL
180 targets, including those with *C11orf53*, is not specific, but rather exacerbated in this cluster.
181 To test this, we sought to divide samples by genotype at rs3087967, the variant associated
182 with expression changes of trans-eQTL targets (Vaughan-Shaw *et al.,* 2021), and analyse the
183 congruence of trans-eQTL target expression relatedness within clusters. While genotype

184 information was unavailable for the Smillie *et al.,* (2019) dataset, raw sequencing reads were
185 available for the Elmentaite *et al.,* (2021) dataset and as rs3087967 lies within the 3' UTR of
186 *C11orf53*, we performed variant calling on these samples using orthogonal tools,
187 Supplementary Table 4. Using freebayes (Garrison & Marth, 2012), we found that all samples
188 were called as homozygous for the non-risk allele at rs3087967, except for one sample called
189 as heterozygous. However, as all 3 other samples from this individual were called as
190 homozygous non-risk, it is likely this is a technical error. Using bcftools (Danecek et al., 2021),
191 all samples were identified to be homozygous non-risk for rs3087967. The lack of genetic
192 variation at rs3087967 in these samples is consistent with the absence of heightened
193 *C11orf53* variability in cluster 18 and indicates this dataset would be unlikely to be of use to
194 identify *C11orf53*-related expression dynamics. The relatively high variability of trans-eQTL
195 target expression within cluster 18 may be indicative of non-11q23.1-related dynamics, such
196 as changes during differentiation or cell cycle progression.
197
198 To test the potential efficacy of the Smillie *et al.,* (2019) dataset to further study the 11q23.1
199 eQTL target expression dynamics, we compared the standardized variability of 11q23.1 trans-
200 eQTL targets within the respective demarcated clusters at the single-cell level, Supplementary
201 Table 5. We found that the expression variability of 14 of the 15 11q23.1 trans-eQTL targets,
202 expressed in both Elmentaite *et al.,* (2021) cluster 18 and Smillie *et al.,* (2019) cluster 11, was
203 substantially increased in the latter (fold-change range 1.46-9.7, median=1.97, mean=2.83,
204 95% confidence interval=1.50-4.18). The only 11q23.1 trans-eQTL target not to exhibit
205 increased variability in Smillie *et al.,* (2019) cluster 11 was OGDHL (fold change=0.73).
206 Notably, the expression of *C11orf53,* was also greater in Smillie *et al.,* cluster 11 (fold
207 change=1.94). Subsequent analysis was therefore focussed on the Smillie *et al.,* (2019)
208 dataset.
209
210 To divide samples into high and low expressors of *C11orf53*-expression related genes, we
211 hierarchically clustered samples based on the relative expression of pseudo-bulk WGCNA-
212 identified blue module hub genes. Hub genes were defined by module membership > 0.7,
213 intramodular connectivity > 0.7 and network adjacency > 0.3 and include 10 genes: *TRPM5,*
214 *PSTPIP2, SH2D6, ALOX5, BMX, GNG13, SH2D7, HCK, PLCG2, MATK*, Figure 4A. Five
215 samples were separated at the first branch of clustering and exhibit a strong relative reduction
216 in the expression of these genes. This grouping of samples is henceforth referred to as the
217 'blue module hub gene grouping'. To assess the significance of this separation at representing

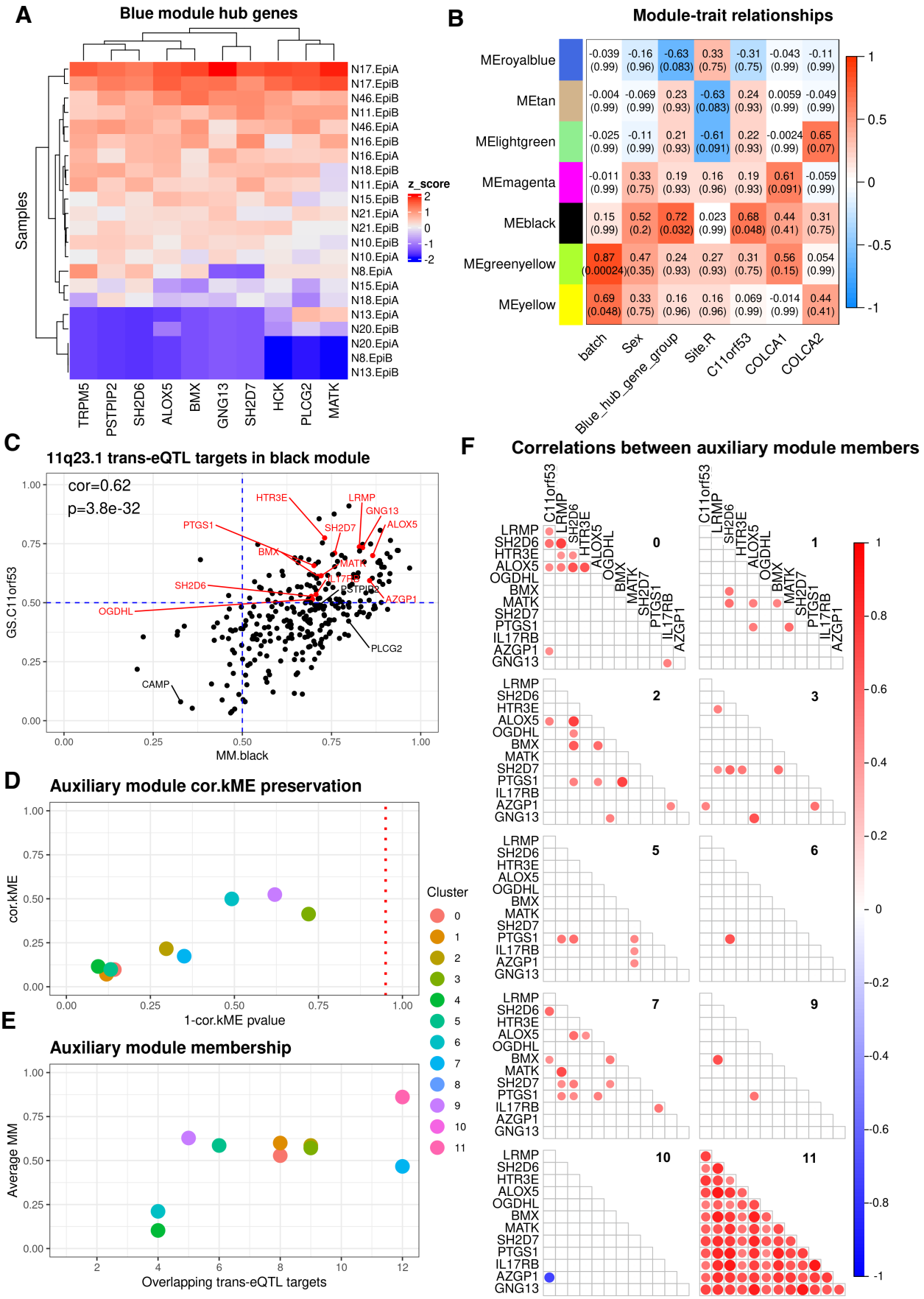
A
Blue module hub genes
Samples
N17.EpiA
N17.EpiB
N46.EpiB
N11.EpiB
N46.EpiA
N16.EpiB
N16.EpiA
N18.EpiB
N11.EpiA
N15.EpiB
N21.EpiA
N21.EpiB
N10.EpiB
N10.EpiA
N8.EpiA
N15.EpiA
N18.EpiA
N13.EpiA
N20.EpiB
N20.EpiA
N8.EpiB
N13.EpiB
TRPM5
PSTPIP2
SH2D6
ALOX5
BMX
GNG13
SH2D7
HCK
PLCG2
MATK
z_score
2
1
0
-1
-2
B
Module-trait relationships
MEroyalblue
MEtan
MElightgreen
MEmagenta
MEblack
MEgreenyellow
MEyellow
-0.039 (0.99) -0.16 (0.96) -0.63 (0.083) 0.33 (0.75) -0.31 (0.75) -0.043 (0.99) -0.11 (0.99)
-0.004 (0.99) -0.069 (0.99) 0.23 (0.93) -0.63 (0.083) 0.24 (0.93) 0.0059 (0.99) -0.049 (0.99)
-0.025 (0.99) -0.11 (0.99) 0.21 (0.93) -0.61 (0.091) 0.22 (0.93) -0.0024 (0.99) 0.65 (0.07)
-0.011 (0.99) 0.33 (0.75) 0.19 (0.93) 0.16 (0.96) 0.19 (0.93) 0.61 (0.091) -0.059 (0.99)
0.15 (0.99) 0.52 (0.2) 0.72 (0.032) 0.023 (0.99) 0.68 (0.048) 0.44 (0.41) 0.31 (0.75)
0.87 (0.00024) 0.47 (0.35) 0.24 (0.93) 0.27 (0.93) 0.31 (0.75) 0.56 (0.15) 0.054 (0.99)
0.69 (0.048) 0.33 (0.75) 0.16 (0.96) 0.16 (0.96) 0.069 (0.99) -0.014 (0.99) 0.44 (0.41)
batch
Sex
Blue_hub_gene_group
Site.R
C11orf53
COLCA1
COLCA2
1
0.5
0
-0.5
-1
C
11q23.1 trans-eQTL targets in black module
cor=0.62
p=3.8e-32
HTR3E
LRMP
GNG13
ALOX5
SH2D7
PTGS1
BMX
MATK
SH2D6
IL17RB
PSTPIP2
AZGP1
OGDHL
PLCG2
CAMP
GS.C11orf53
MM.black
D
Auxiliary module cor.kME preservation
cor.kME
1-cor.kME pvalue
Cluster
0
1
2
3
4
5
6
7
8
9
10
11
E
Auxiliary module membership
Average MM
Overlapping trans-eQTL targets
F
Correlations between auxiliary module members
C11orf53
LRMP
SH2D6
HTR3E
ALOX5
OGDHL
BMX
MATK
SH2D7
PTGS1
IL17RB
AZGP1
GNG13
0
1
2
3
5
6
7
9
10
11

Figure 4. Several 11q23.1 trans-eQTL targets comprise *C11orf53*-correlated network in tuft-like cluster only. (A) Relative (z-score) expression of blue module hub genes from Fig.1D (MM>0.7, kIM>0.7, adj > 0.3). Robustness assessed by 10,000 permutations: p=0.055. (B) Module trait matrix of gene modules identified by WGCNA within pseudo-bulked expression from cluster 11. Only modules exhibiting a correlation with a covariate (FDR<0.1) are shown. Total number of modules=20. (C) Correlation of Gene Significance (GS) and Module Membership (MM) of genes in the black module from (B). 11q23.1 trans-eQTL targets are highlighted. 11q23.1 trans-eQTL targets with GS.C11orf53 > 0.5 and MM.black > 0.5 (red) were used as the auxiliary module. (D) Preservation of correlations between auxiliary module genes with the module eigengene (ME) and equivalent values in cluster 11. Dashed line indicates nominal significance threshold (p=0.05). (E) Average MM of genes within the auxiliary module across clusters. (F) Pairwise pearson correlations (p<0.05) between the pseudo-bulked expression of auxiliary module genes across clusters. Cluster number in upper right of each facet. Cluster 4 and 8 exhibited no significant correlations and so are not plotted.

underlying transcriptional differences, we performed 10,000 permutations, using 10 randomly sampled genes, and generated a p-value of 0.055.

To first test gene-gene relatedness within cluster 11, we performed WGCNA on the relative, pseudo-bulked expression of the top 5000 most variable genes within this cluster, identifying a total of 20 modules, 7 of which exhibited correlations with sample covariates that approached significance (FDR<0.1), Figure 4B. We found one module, 'cluster 11 black', which was highly correlated with both the 'blue hub gene grouping' (cor=0.72, FDR=0.032) and *C11orf53* expression (cor=0.68, FDR=0.048). 'Cluster 11 black' is comprised of 290 genes, including fifteen 11q23.1 trans-eQTL targets, Additional File 3. As the 'blue module hub gene' grouping is derived from analysis of genes correlated with *C11orf53* across all cells, the correlation of 'cluster 11 black' with both this grouping and *C11orf53* expression indicates that this relationship is preserved within and potentially derived from this cell-cluster.

We then wanted to test whether the gene-gene relatedness of 11q23.1 trans-eQTL targets, correlated with *C11orf53*, was specific to cluster 11. To this end, we defined an auxiliary module, comprised of the twelve 11q23.1 trans-eQTL targets correlated with *C11orf53* (cor>0.5, p<0.05) in cluster 11 black, which exhibited high module membership (MM.black > 0.5), Figure 4C. These genes include: *HTR3E, LRMP, GNG13, ALOX5, SH2D7, PTGS1, MATK, BMX, AZGP1, IL17RB, SH2D6* and *OGDHL.* We performed pairwise module preservation of this auxiliary module, using identical parameters as used for intra-cluster 11 analysis, in all other clusters, see Methods. For two modules, cluster 8 and cluster 10, the 5000 most variable genes included only a single member of the auxiliary module and so were excluded from this analysis. To analyse the preservation of the connectivity of these genes, we assessed the similarity of each gene correlation with the module eigengene, and the

244 equivalent values in cluster 11 (cor.kME), Figure 4D. No module exhibited a significant
245 cor.kME with cluster 11 ($p>0.05$), indicating there is low overall preservation of the connectivity
246 between these genes in all other clusters. The average module membership of genes in this
247 module (average.MM) was also reduced in all clusters compared with cluster 11, Figure 4E.
248 Finally, we analysed the pairwise gene-gene correlations between all members of the auxiliary
249 module and *C11orf53* within each cluster, Figure 4F. While there are rare correlations between
250 these genes in other modules (cor>0.5, $p<0.05$), all comparisons reach this threshold in cluster
251 11. Taken together, this evidence indicates these 12 trans-eQTL targets comprise a
252 transcriptional network that is correlated with *C11orf53* expression and likely specific to cluster
253 11.
254
255 ***Identification of cluster 11 abundance associated genes***
256
257 As many of the 11q23.1 eQTL targets, including those comprising the cluster 11-specific
258 network, demarcate this cluster, we wanted to examine the relationship between their
259 expression and cluster 11 abundance. First, we performed linear modelling of the relative
260 abundance of cluster 11 and the pseudo-bulked expression of *C11orf53* only. We found that
261 the expression of *C11orf53* is associated with the relative abundance of cluster 11
262 (coefficient=0.389, $p=0.00431$) indicating potential for the expression of *C11orf53* alone to be
263 moderately predictive of the abundance of this cell-type, Figure 5A.
264
265 To agnostically test the predictive power of 11q23.1 trans-eQTL target expression on cluster
266 11 abundance, we tested the association between the expression of all genes and the
267 proportion of cluster 11 in samples, Figure 5B. We found that all genes significantly associated
268 with the abundance of this cluster (FDR<0.05, log-fold change>1) were indeed 11q23.1 trans-
269 eQTL targets, including: *ALOX5, BMX, GNG13, MATK, SH2D7, PSTPIP2, TRPM5* and
270 *PTGS1.* In fact, the strength of gene association with cluster 11 abundance was also
271 significantly enriched for 11q23.1 trans-eQTL targets (NES=2.15, $p=8.03e-10$, Figure 5C).
272
273 While our linear modelling strongly supports a predictive role of 11q23.1 eQTL target
274 expression in the abundance of cluster 11, we wanted to agnostically test whether the
275 expression of the *C11orf53*-related trans-eQTL targets was correlated with abundance
276 changes to any cluster. To this end, we utilised miloR (Dann et al., 2021) to calculate cell-
277 neighbourhoods, Supplementary Figure 5, which were then used to perform differential
278 abundance testing across the 'blue module hub gene grouping', defined in Figure 4A. To

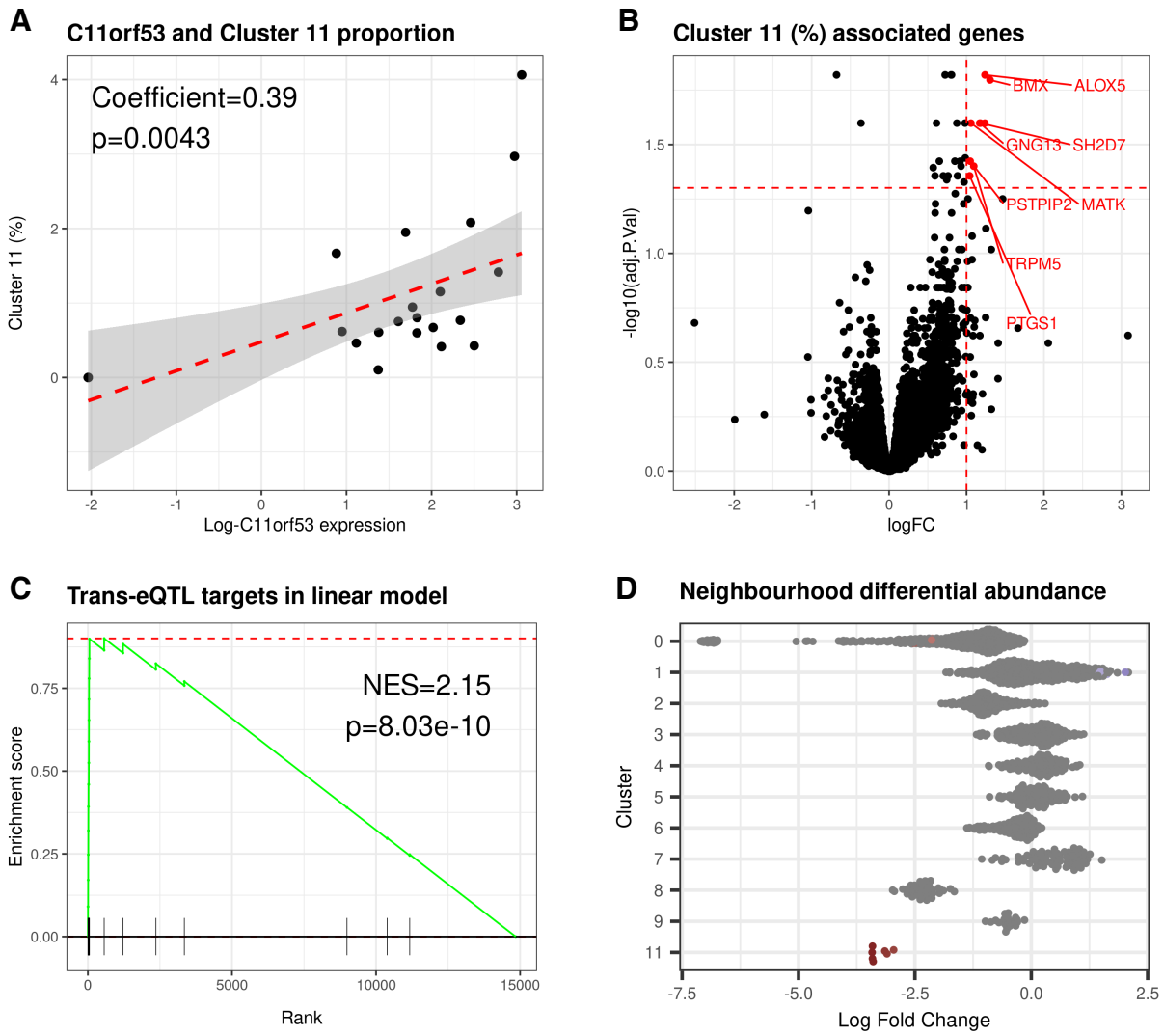

Figure 5. 11q23.1 trans-eQTL target expression is associated with the abundance of tuft cell-like cluster. (A) Linear modelling of pseudo-bulked *C11ORF53* expression and cluster 11 abundance. (B) Volcano plot of linear model result on pseudo-bulked expression of all 14,843 genes. Significantly associated 11q23.1 trans-eQTLs (logFC>1, FDR<0.05) highlighted. (C) GSEA of 11q23.1 trans-eQTLs (FDR<0.05) in (B), ranked by logFC. (D) Differential abundance of neighbourhoods in the 'Low' blue hub gene group compared to 'High'. Neighbourhoods were identified using miloR (Dann *et al.,* 2021) and grouped by cluster. Only significant neighbourhoods with major cluster proportion > 0.8 are plotted and only significant neighbourhoods (Spatial FDR < 0.01) are coloured by their logFC (red=down, blue=up). No neighbourhoods from cluster 10 were comprised of major proportion > 0.8.

generalise neighbourhoods to the cell clusters we have identified, we subsequently filtered for neighbourhoods which represented a majority of a single cluster (majority proportion > 0.8) Figure 5D. No neighbourhood from cluster 10 was comprised of a majority proportion of 0.8 and so this cluster was not included. In the low *C11orf53*-related gene expressing samples there are significant reductions (Spatial FDR < 0.01) from cluster 0 and increases in neighbourhoods in clusters 1, Figure 5D. The change in abundance of these neighbourhoods represent a small proportion of the total number of neighbourhoods detected in these clusters (2.1% and 1.3% respectively) and are therefore unlikely to represent a dramatic phenotype.

287 In contrast, all 7 of the neighbourhoods comprising a majority of cluster 11 cells were
288 significantly underrepresented in the low 'blue module hub gene group'. These results indicate
289 11q23.1 eQTL target expression is correlated with a significant and likely specific change in
290 abundance of cluster 11 cells.
291
292 **Discussion**
293
294 In this study, our pan-cluster WGCNA serves as validation of the expression relatedness
295 between trans-eQTL targets previously identified to be correlated with CRC associated
296 variation at 11q23.1 (Vaughan-Shaw *et al.,* 2021). 11q23.1 trans-eQTL target expression was
297 also found to be more correlated with *C11orf53* over other cis-eQTL targets. Following
298 clustering of single cells, many of the genes demarcating a single cluster, number 11, were
299 found to be 11q23.1 trans-eQTLs targets. Enrichment of these markers against putative gene
300 sets showed cluster 11 transcriptionally resembled tuft cells, replicated in an independent
301 dataset. WGCNA within cluster 11 identified several 11q23.1 trans-eQTL targets that exhibited
302 a high level of relatedness, subsequent analysis of the preservation of this relatedness
303 indicated this was likely to be specific to this cell cluster. Finally, samples which exhibited low
304 overall expression of 11q23.1 trans-eQTL targets most correlated with one another, were
305 found to exhibit a specific and dramatic reduction of the tuft cell-like cluster. Therefore, our
306 results potentiate CRC risk associated variation at 11q23.1 reduces the abundance of colonic
307 tuft cells.
308
309 To our knowledge, this is the first study to map CRC risk associated eQTL targets to specific
310 epithelial cell-types. Heritable inflammatory bowel disease risk loci have recently been
311 associated with shifts in transcriptional dynamics in individual colonic epithelial cells (Smillie
312 et al., 2019) and it is possible that other CRC risk variants, with robust eQTL effects, are
313 associated with cell-specific changes in transcriptional dynamics. Delineating the cell-specific
314 expression of CRC risk-associated eQTLs may provide valuable insights into the mechanism
315 of risk-associated pathophysiology and should be a focus of future work. The growing size
316 and availability of scRNAseq datasets will likely make cell-specificity mapping of heritable
317 disease associated eQTLs significantly easier and available, particularly if genotype data is
318 available. Indeed, our study is also not the first use of WGCNA to detect gene-gene
319 relatedness in scRNAseq data. WGCNA has been utilised to identify gene modules associated
320 with the activation of neuronal stem cells (Luo et al., 2015) and human induced pluripotent

stem cells (Wu et al., 2021), however, like our own study, these studies did not utilise expression from individual cells as the input for WGCNA.

Surprisingly, the expression of the vast majority of 11q23.1 eQTL targets mapped to the cell-type that transcriptionally resembles tuft cells, including; *LRMP, IL17RB, SH2D6, PLCG2, PSTPIP2, TRPM5, SH2D7, AXGP1, PTGS1, ALOX5, BMX*. Many of the most significant 11q23.1 trans-eQTL targets, such as *LRMP, SH2D7* and *ALOX5*, have not previously been associated with specific expression in this cell-type, potentiating their status as a marker in the colonic epithelium. Additional markers of the tuft cell-like cluster include *HCK* and *HPGDS,* for which there is some orthogonal evidence of expression within tuft cells (Gerbe et al., 2011; Yamaga et al., 2018). This improves our confidence that cluster 11 represents this cell-type and is not an artefact of the analysis.

It is noteworthy that many of the genes with expression found to be in association with *C11orf53* in the scRNAseq data were indeed identified as trans-eQTL targets in the bulk analysis (Vaughan-Shaw et al., 2021). While the mapping of the expression of these genes to a tuft-like cell cluster could only be achieved by using expression from individual cells, the prior identification of these genes by bulk analysis is a testament to the power of such approaches, and concordance of their findings with single cell-based methods.

Finally, the overall potentiation of tuft cell perturbation is of great interest regarding characterisation of the mechanism governing CRC risk at 11q23.1. Tuft cells are associated with stem-, neuro-transmitting and immune-related functions (Banerjee et al., 2020; Gerbe et al., 2016; Middelhoff et al., 2017; Yi et al., 2019), however much of the evidence regarding their function is derived from other organs and cannot necessarily be extrapolated to the colon. Interestingly, genetic ablation of tuft cell abundance has been associated with exacerbated tumour progression in mouse models of pancreatic cancer (DelGiorno et al., 2020; Hoffman et al., 2021). Both studies show this is likely in association with perturbed immune cell function and signalling. In line with this, tuft cell abundance has recently been shown to be reduced in quiescent ulcerative colitis patients (Kjærgaard et al., 2021), suggesting tuft cells are involved in immune regulation in the colon. Future work should aim to experimentally validate the relationship between 11q23.1 variation and tuft cell abundance, examine how this impacts tumourigenesis and identify the potential mechanism of CRC risk predisposition.

356 **Materials and methods**

357

358 ***Availability of data and materials***

359

360 Raw gene-level expression counts of healthy colonic epithelial cells, published by Smillie *et*
361 *al.,* (2019), were obtained from Single Cell Portal using accession code SCP259. Samples
362 from one patient, N51, were removed as they were found to be outliers on the basis of cell-
363 level mitochondrial and ribosomal protein gene expression, in addition to principal component
364 analysis of pseudo-bulked expression. Fastq files for the second dataset, published by
365 Elmentaite *et al.,* (2021) were obtained from https://www.ebi.ac.uk/arrayexpress, using
366 accession code E-MTAB-9543. Fastq files were aligned to the hg19 transcriptome using the
367 10X Genomics Cell Ranger v3.02 pipeline (Zheng et al., 2017) to produce the raw gene-level
368 counts. All code used for the analysis performed in this study is available at
369 https://github.com/BradleyH017/Harris_et_al_WGCNAscRNA.

370

371 ***Pre-processing, dimensionality reduction and clustering of scRNAseq data***

372

373 All subsequent expression analysis was completed in R version 4.0.2 (R Core Team, 2020).
374 Once raw counts had been obtained for both datasets, bad quality droplets were filtered by a
375 series of quality control steps: i) potential empty droplets were detected by thresholding at the
376 inflection point of the barcode rank plot of cells, calculated using *DropletUtils* v1.8.0 (Griffiths
377 et al., 2018), ii) genes expressed in fewer than 20 cells were removed, iii) cells with an
378 expression sparsity > 0.99 were removed, iv) cells with proportion of mitochondrial gene
379 expression greater than 2.5*(median absolute deviation) from the median proportion were
380 removed.

381

382 Following filtration, counts were loaded into a Seurat object using Seurat v4.0.1 (Hao et al.,
383 2021). Initial clustering was performed using Seurat's reciprocal PCA method of batch
384 correction with *SCTransform* as per Hao *et al.,* (2021) guidelines
385 (https://satijalab.org/seurat/articles/integration_rpca.html). The processed Seurat object was
386 first split by sample and data integration was performed on the first 50 principal components.
387 The principal components of the integrated data were then calculated, which was used to
388 calculate the UMAP embedding for all cells, based on 50 principal components

389

390 To identify clusters, a nearest neighbour graph was constructed on the integrated data, using
391 50 principal components. Clusters were then identified via the *FindClusters* function using a
392 resolution of 0.6. For the Smillie *et al.,* (2019) data analysis, we utilised a k value of 250, as
393 this is concordant with the authors analysis and provided the greatest confidence in
394 identification of clusters than other k values. Concordance was tested by enrichment against
395 the authors cluster markers; data not shown. For the Elmentaite *et al.,* (2021) analysis, we
396 utilised a k value of 20. Any value greater than this resulted in failure to detect the tuft-cell
397 resembling cluster.
398
399 To identify potential doublets in the filtered dataset, we utilised *DoubletFinder* v2.0.3
400 (McGinnis et al., 2019) as per the authors guidelines (https://github.com/chris-mcginnis-
401 ucsf/DoubletFinder). The fully filtered dataset was then re-used as input for integration,
402 dimensionality reduction and clustering as described above.
403
404 To test the robustness of the clusters we identified, we performed pairwise differential gene
405 expression analysis by a receptor operator curve test using Seurat's *FindMarkers* function. In
406 order to only merge clusters which were extremely similar, without over-clustering, we defined
407 similar clusters as those with less than 30 differentially expressed genes with area under the
408 curve score of 0.6 differentiating them. We found no clusters that fall below this threshold and
409 so did not modify our initial clustering in either dataset.
410
411 ***Pan-cluster WGCNA***
412
413 To analyse correlation of gene expression across all cells from the filtered Smillie *et al.,* (2019)
414 data, we first subset for the nominally significant 11q23.1 trans-eQTLs previously reported
415 (Vaughan-Shaw et al., 2021). The relative pseudo-bulked expression was then calculated by:
416 i) summing reads for each gene across all cells within samples, ii) recombining the summed
417 reads into a non-normalised bulk matrix, iii) log normalising using TMM normalised size factors,
418 calculated using *edgeR* v3.32.1 (McCarthy et al., 2012). Log-TMM normalised bulk expression
419 was then z-scored across genes before analysis.
420
421 To perform the network analysis, we used *WGCNA* v1.69 (Langfelder & Horvath, 2008). First,
422 *C11orf53*, *COLCA1* and *COLCA2* pseudo-bulk expression was extracted. A soft threshold of
423 14 was then selected after computation of mean connectivity and scale free topology, using
424 the recommended 'powerEstimate'. A signed adjacency matrix was then calculated, which

425 was subsequently used to calculate a topological overlap matrix (TOM). Modules were defined
426 by using a dynamic tree cut of hierarchically clustered gene expression by average distances.
427 We did not find any modules with a height of module separation below 0.25 and so did not
428 merge any module. Module eigengenes were then calculated and their correlation with
429 binarized sex, batch, site, and relative, pseudo-bulked expression of *C11orf53, COLCA1* and
430 *COLCA2* was then assessed. Correlation p-values were multiple testing corrected by the
431 Benjamini-Hochberg method (Benjamini & Hochberg, 1995). To visualise the blue module
432 hub genes, a network object was generated from the TOM of blue module genes using
433 *network* v1.17.1 (Butts, 2008). Non-connected genes, along with adjacencies < 0.3, were then
434 removed and remaining genes were plotted using *ggplot2* v3.3.5 (Wickham, 2009).
435
436 ***Gene set enrichment analysis***
437
438 All gene set enrichment analysis was carried out using R package fgsea v1.14.0 (Korotkevich
439 et al., 2021). Genes were ranked by their module membership, gene significance for *C11orf53*
440 expression, or log fold change of differential expression as stated. In the case where multiple
441 gene sets were being tested, i.e cluster 11 markers against all Smillie et al., putative markers,
442 p-values were multiple testing corrected by the false discovery rate method.
443
444 ***Calculation of cluster markers***
445
446 To calculate the markers of each of our own and the Smillie *et al.,* (2019) clusters, we first
447 generated a log-transcripts per 10,000 expression matrix for the expression of genes within
448 each cell. This was done so that markers could be calculated using expression values that
449 were not affected by the relative expression of genes within this dataset and so were more
450 applicable to future use. Markers were identified by differential expression of genes within
451 each cluster and all other clusters combined, using MAST v1.160 (Finak et al., 2015).
452
453 ***Analysing the variability of trans-eQTL targets within clusters***
454
455 To analyse the variability of the expression of 11q23.1 trans-eQTL targets within each cluster,
456 we applied the pseudo-bulking approach described in *Pseudo-bulk WGCNA* to each cluster
457 independently. To make expression variability comparable across samples and clusters, the
458 expression was z-scored across samples.
459

460 To analyse expression variability at the single level, we utilised Seurat's *FindVariableFeatures*
461 function and variance stabilising transformation. In concordance with the identification of many
462 trans-eQTL targets identified as markers, their mean expression was very low in several
463 clusters within each dataset. For within dataset comparison of variance, we therefore utilised
464 the raw variance, not normalising for mean expression. For the between dataset comparison
465 of variance, we utilised the normalised variance values.
466
467 ***Genotyping of Elmentaite et al.,* (2021) *samples***
468
469 To identify the rs3087967 genotype of Elmentaite *et al.,* (2021) samples, we utilised two
470 variant calling approaches. These were chosen on the basis of findings from a recent review
471 which identified these methods as the most sensitive for this purpose (Liu et al., 2019).
472 Freebayes (Garrison & Marth, 2012) was used with default settings, genotyping over a 10bp
473 region including rs3087967. Bcftools variant calling (Danecek et al., 2021) was performed on
474 chromosome 11 using a minimum base quality of 30, disabling read-pair overlap detection
475 and not discarding anomalous pairs.
476
477
478 ***Sample group definition***
479
480 In the absence of genotype data for Smillie *et al.,* (2019) patients, we grouped samples into
481 high and low expressors of a *C11orf53*-associated signature by defining the hub genes of the
482 pseudo-bulk WGCNA blue module. These were defined by a module membership (MM) > 0.7,
483 intramodular connectivity (kIM) > 0.7 and network adjacency > 0.3. Samples were then
484 hierarchically clustered by their relative pseudo-bulked expression of these genes using
485 complete distance. We tested the robustness of our sample grouping by bootstrapping,
486 selecting 10 random genes 10,000 times, and counting the number of times this exact
487 separation was achieved – which was 550 times.
488
489 ***Intra-cluster WGCNA***
490
491 To agnostically identify gene-gene relatedness within cluster 11, we performed WGCNA as
492 described (see *Pseudo-bulk WGCNA*), selecting only the 5000 most variable genes using
493 Seurat's *FindVariableFeatures* and variance stabilising transformation. The scale free

494 topology threshold utilised was 6, as per the 'power estimate'. P-values were corrected for
495 multiple testing as before.
496
497 ***Module Preservation Analysis***
498
499 To analyse the preservation of the relatedness of *C11orf53*-correlated 11q23.1 trans-eQTL
500 targets, we defined an auxiliary module, comprised of the 12 trans-eQTL targets correlated
501 with *C11orf53* expression (cor>0.5, p<0.05) within the 'cluster 11 black' module. Pseudo-
502 bulked expression of each cluster was calculated and subset for the 5000 most variable genes
503 as before, see *Pseudo-bulk WGCNA* and *Intra-cluster WGCNA*. The expression from each
504 cluster was then raised to the same scale free topology threshold as cluster 11. The
505 preservation of all modules, including the auxiliary module, was calculated in a pairwise
506 manner with cluster 11, following the tutorial by Langfelder & Horvath (2008)
507 (https://horvath.genetics.ucla.edu/html/CoexpressionNetwork/ModulePreservation/Tutorials/).
508 To summarise module preservation results, we extracted cor.kME values – a measure of the
509 similarity of auxiliary module genes with the auxiliary module eigengene, and equivalent
510 results from cluster 11. We also extracted the nominal p-value for this correlation
511 (log.p.cor.kME), which was subsequently un-logged. The mean connectivity of auxiliary
512 module genes with the module eigengene was also calculated within each cluster. Pairwise
513 correlations (p<0.05) between the expression of the auxiliary module genes with one another
514 and *C11orf53* expression were plotted using corrplot (Wei & Simko, 2017).
515
516 ***Linear modelling of cluster abundance and pseudo-bulked gene expression***
517
518 Univariate linear modelling of cluster 11 abundance was performed on the TMM normalised,
519 non-z-scored pseudo-bulked expression matrix, so that results are more relevant to further
520 study. We fitted a linear model to all genes and performed empirical Bayes moderation using
521 *limma* v3.46.0 (Ritchie et al., 2015). P-values were adjusted by Benjamini-Hochberg multiple
522 testing correction (Benjamini & Hochberg, 1995).
523
524 ***Differential abundance testing***
525
526 Differential abundance testing was performed using miloR v0.99.8 (Dann et al., 2021). To
527 mitigate any potential for package-specific artefacts of the analysis, we first re-generated the
528 k nearest neighbour graph using 250 nearest neighbours from the integrated expression. The

graph was then built using 4 PCA components. Differential abundance testing was carried out using a Quasi-Likelihood F-test on TMM normalised cell proportions. Differentially abundant neighbourhood results were then annotated for their majority cluster proportion and those comprised of fewer than 80% of the majority cluster were removed.

Author contributions

Conceptualisation: BTH, VR, MGD, SMF

Methodology: BTH, VR, SMF, MGD, AO, JPB, KD, MT, PGVS

Investigation: BTH

Original draft writing: BTH

Review & Editing: BTH, VR, JPB, KD, MT, AO, MGD, SMF

Funding Acquisition: SMF, MGD, FVND

Supervision: VR, MGD, SMF

Supplementary Material

Subject ID	Status	Location	Gender
N8	Healthy	#N/A	Female
N10	Healthy	Right_Colon	Female
N11	Healthy	Right_Colon	Male
N13	Healthy	Right_Colon	Female
N15	Healthy	Right_Colon	Male
N16	Healthy	Right_Colon	Male
N17	Healthy	Transverse_Colon	Male
N18	Healthy	Transverse_Colon	Female
N20	Healthy	#N/A	Female
N21	Healthy	Left_Colon	Female
N46	Healthy	Right_Colon	Male

Supplementary Table 1. Smillie *et al.,* (2019) patient metadata

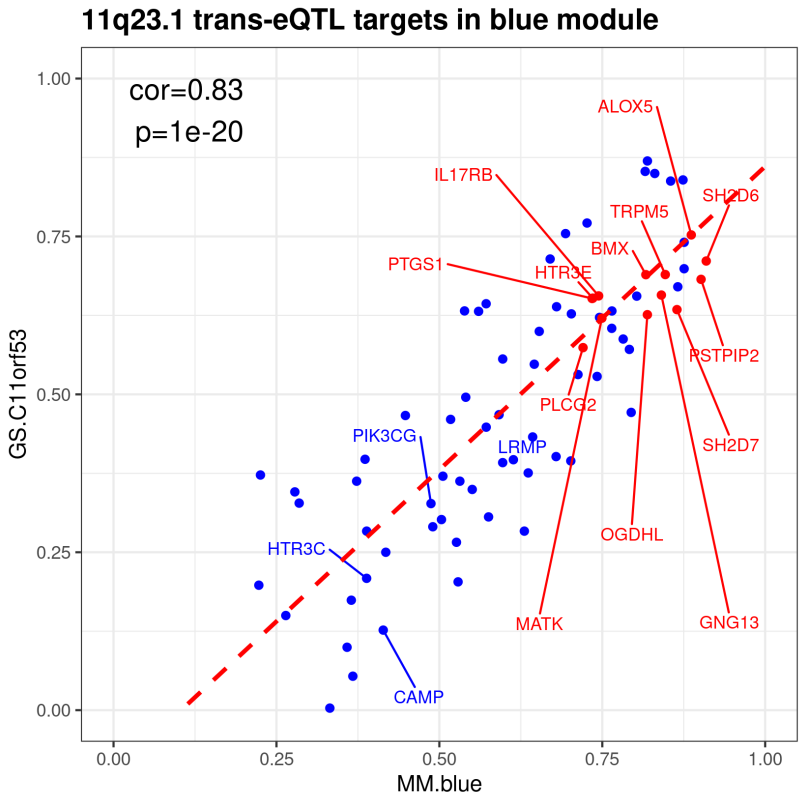

Supplementary Figure 1. Correlation of Module Membership (MM) and Gene Significance (GS) for *C11orf53* expression in the blue module. 11q23.1 trans-eQTL targets are highlighted, red if MM.blue and GS.C11orf53 > 0.5.

Gene_symbol	GS.C11orf53	p.GS.C11orf53
MFSD7	0.869516061	1.49E-07
P2RY2	0.852996421	4.57E-07
FANK1	0.849691779	5.63E-07
LINC00261	0.839485426	1.04E-06
KLK4	0.837697653	1.15E-06
PLEKHG4	0.771254176	2.65E-05
RNF32	0.754523148	4.97E-05
ALOX5	0.752415106	5.36E-05
PTPRD	0.740741398	8.05E-05
ASTE1	0.714297945	0.000188259
SH2D6	0.71110102	2.07E-04
HCK	0.698902984	2.96E-04
TRPM5	0.689672239	3.84E-04
BMX	0.689502913	3.85E-04
PSTPIP2	0.682088126	4.71E-04
MYOM1	0.670290717	6.42E-04
GNG13	0.657207652	8.90E-04
IL17RB	0.655879017	0.000918972
CYR61	0.655513165	0.000927169
HTR3E	0.652281	0.001002333
PTGS1	0.651790925	0.001014171
WWP2	0.643465569	0.001234253
FYB	0.638720231	0.001376965
SH2D7	0.63416094	0.001527043
SNRPA	0.632098175	0.00159937
AC025335.1	0.632010561	0.001602506
RAI1	0.631424527	0.001623611
MARCKSL1	0.627445473	0.001773235
OGDHL	0.626140466	0.00182478
CRYM	0.621805521	0.002005201
MATK	0.620641028	0.002056158
ALOX5AP	0.604524135	0.002881786
RP11-315O6.1	0.599692821	0.003177792
MSLN	0.587571695	0.004034646
PLCG2	0.573987877	0.005216381
SCRN1	0.571174034	0.005494069
CD96	0.555950868	0.007218247
L3MBTL1	0.547690051	0.008327128
RP11-1220K2.2	0.531364238	0.010932727
IKZF4	0.528361091	0.011477883
FAM65A	0.495417788	0.019052761
GFI1B	0.471411163	0.026778703
SGK223	0.467790056	0.028134237
RNF144A	0.466520671	0.028622119
CHSY1	0.460356935	0.031087422
DKK3	0.448035289	0.036517806
ZFP1	0.432558977	0.044363985
AFAP1L2	0.401466056	0.064037752
TBC1D24	0.397206607	0.067180992
LRMP	0.396518404	0.067699644
PODXL	0.394606685	0.069156315
SLC25A30	0.391914382	0.071247869
ARHGEF3	0.375600915	0.084958526
ARHGEF2	0.372293733	0.087962678
FILIP1L	0.370412873	0.089706055
C20orf194	0.362507448	0.097315042
NOTCH4	0.362506253	0.097316226
ARHGAP31	0.3494408	0.11091913
PGAM4	0.34556863	0.115204208
FGFRL1	0.32779629	0.136419162
PIK3CG	0.327080559	0.137328021
ATF3	0.305953301	0.16612758
PPP1R3B	0.301754652	0.172314946
CAPN9	0.290378683	0.189872811
APH1B	0.283453554	0.201136526
MT1H	0.283442955	0.201154103
GNB5	0.265793153	0.23186717
SNORA31	0.249996893	0.261829995
HTR3C	0.20872	0.351252864
TRIB1	0.203124291	0.364604113
COL1A1	0.197820332	0.377525123
PIP5KL1	0.174089375	0.438438491
CGNL1	0.149829973	0.505720737
CAMP	0.126754067	0.574047366
ISPD	0.099579334	0.659282892
CAPRIN2	0.053739047	0.812256115
DLG5-AS1	0.003234775	0.988601201

Supplementary Table 2. Blue module genes, corresponding Gene Significance for *C11orf53* (GS.C11orf53) and p-value of Gene Significance for *C11orf53* (p.GS.C11orf53). Red=11q23.1 trans-eQTL target (Vaughan-Shaw *et al.,* 2021)

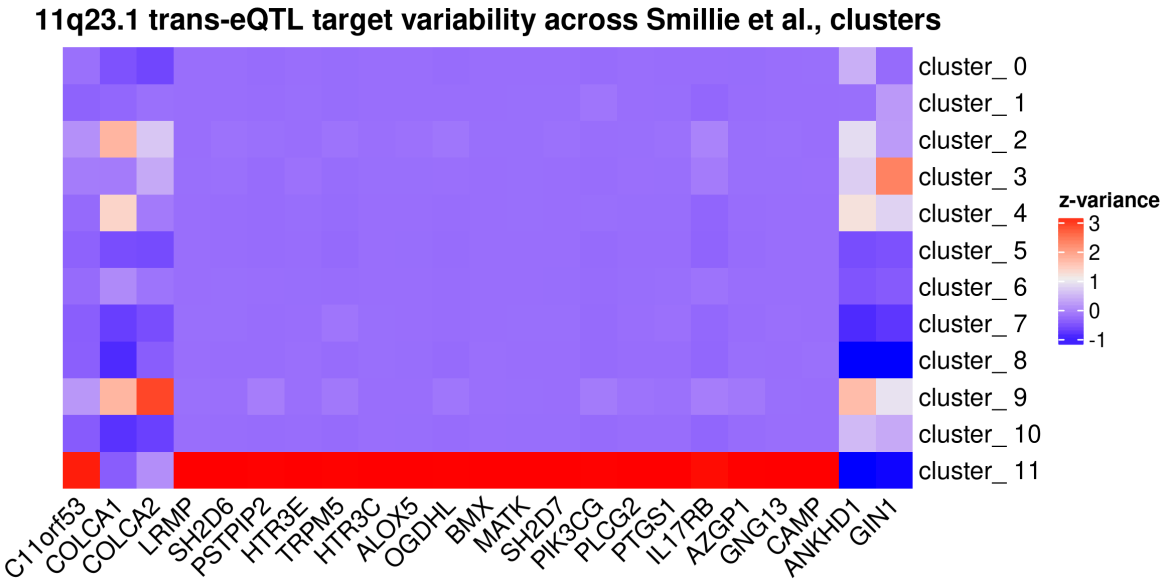

Supplementary Figure 2. Investigating 11q23.1 eQTL target variance at the single cell level. Variance of 11q23.1 eQTL targets across clusters at the single cell level in the Smillie *et al.,* (2019) data. Variance is z-scored within genes.

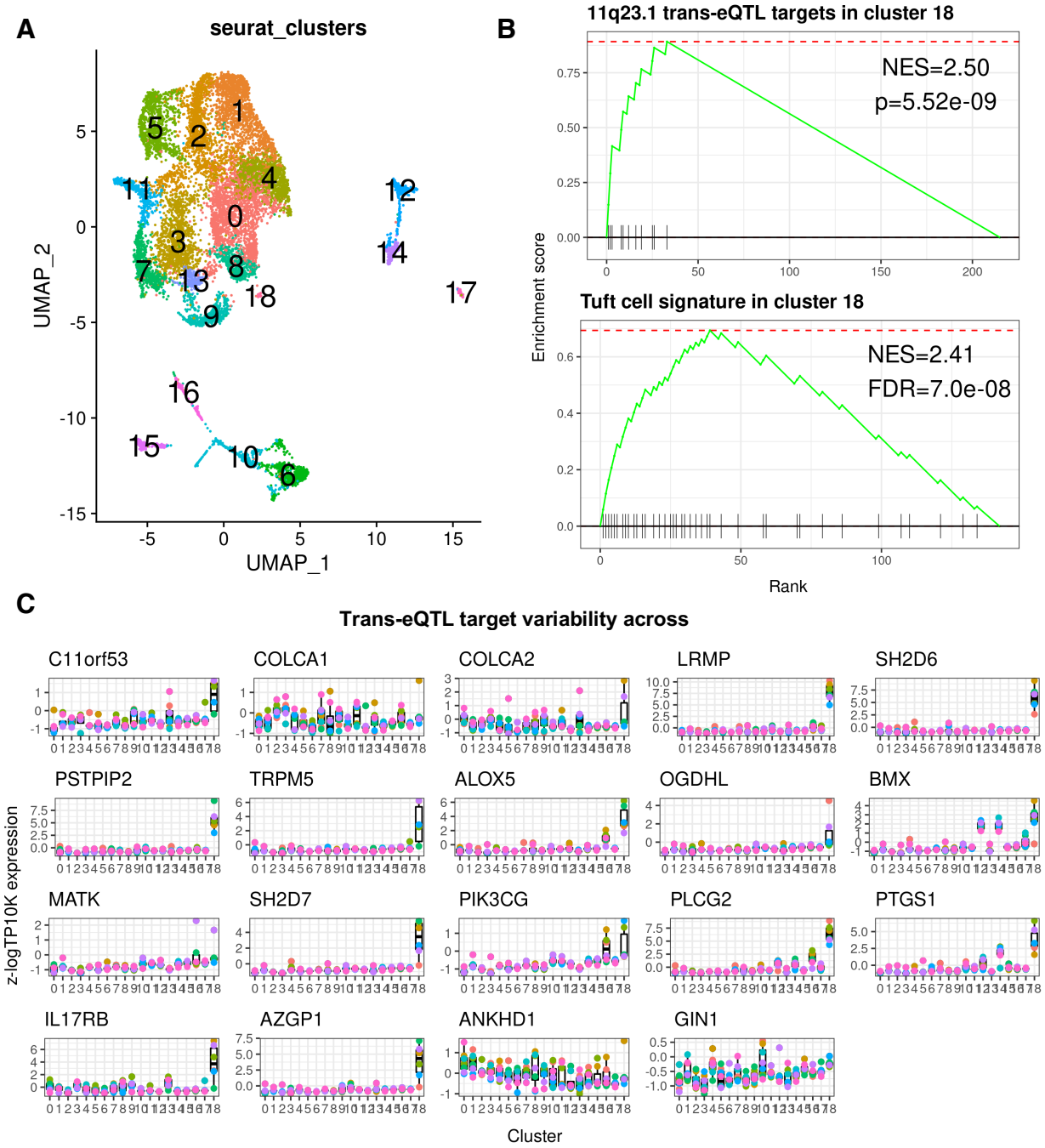

Supplementary Figure 3. Replication of 11q23.1 eQTL expression mapping in independent dataset. (A) UMAP of 11,651 healthy colonic epithelial scRNASeq (Elmentaite *et al.,* 2021). (B) Upper: GSEA of 11q23.1 trans-eQTLs (Vaughan-Shaw *et al.,* 2021; FDR<0.05) in cluster 18. Lower: GSEA of putative colonic tuft cell signature (Smillie *et al.,* 2019) in cluster 18. (D) Relative expression of 11q23.1 trans-eQTLs (FDR<0.05) across clusters.

629

630

631

632

Gene	p_val	avg_log2FC	pct.1	pct.2	p_val_adj
LRMP	2.04E-73	2.614295875	0.903	0.004	3.19E-69
IL17RB	6.17E-69	1.454372429	0.516	0.033	9.64E-65
SH2D6	3.81E-64	2.521466548	0.806	0.002	5.95E-60
PLCG2	1.11E-50	2.182226523	0.71	0.011	1.73E-46
PSTPIP2	1.31E-45	1.656282707	0.581	0.006	2.04E-41
TRPM5	6.51E-44	1.403600676	0.581	0.002	1.02E-39
SH2D7	2.90E-39	1.090698798	0.484	0.001	4.53E-35
AZGP1	9.92E-39	1.061625996	0.452	0.005	1.55E-34
PTGS1	8.37E-30	1.282060245	0.516	0.01	1.31E-25
ALOX5	4.14E-29	1.32717779	0.452	0.004	6.46E-25
BMX	1.08E-22	1.007016149	0.419	0.012	1.68E-18

Supplementary Table 3. 11q23.1 trans-eQTL targets identified as cluster 18 markers from Elmentaite *et al.,* (2021). Markers calculated using MAST (McDavid *et al.,* 2020). Avg_log2FC=average log2 fold change between cluster 11 and all other clusters. Pct1=Proportion of cluster 18 cells expressing gene. Pct2=Proportion of non-cluster 18 cells expressing gene.

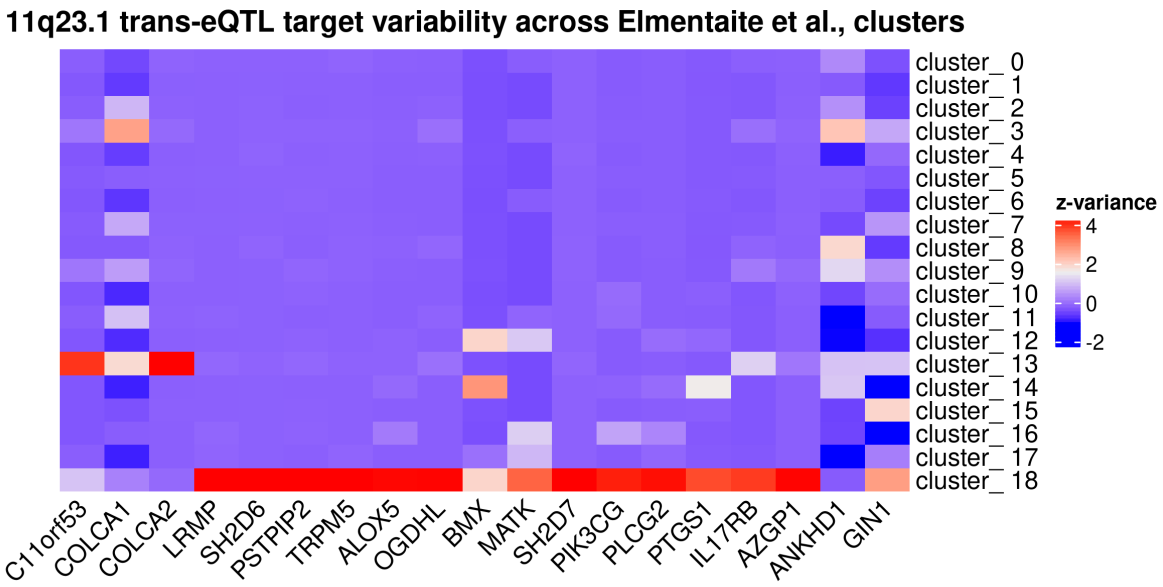

Supplementary Figure 4. Investigating 11q23.1 eQTL target variance at the single cell level. Variance of 11q23.1 eQTL targets across clusters at the single cell level in Elmentaite *et al.,* (2021) data. Variance is z-scored within genes.

Sample	Subject	freebayes_rs3087967	samtools_rs3087967
Human_colon_16S8123908	411C	CC	CC
Human_colon_16S8000473	417C	T/C	CC
Human_colon_16S8000477	417C	CC	CC
Human_colon_16S8000481	417C	CC	CC
Human_colon_16S8000479	417C	CC	CC
Human_colon_16S8000475	417C	CC	CC
Human_colon_16S8002627	432c	CC	CC
Human_colon_16S8002630	432c	CC	CC

Supplementary Table 4. Elmentaite *et al.,* (2019) samples are homozygous non-risk at rs3087967. rs3087967 genotype results of both freebayes (Garrison et al., 2012) and Bcftools (Danecek et al., 2021) variant calling methods. T=colorectal cancer risk allele, C=non-risk allele

Gene	Smillie_cluster11	Elmentaite_cluster18	FC
C11orf53	1.275873075	0.656341714	1.94391587
COLCA1	1.346177989	NA	NA
COLCA2	1.381191066	0.834903033	1.65431315
LRMP	1.695513426	0.173077239	9.79628192
SH2D6	0.518050076	0.196087378	2.64193484
PSTPIP2	0.961252255	0.332407278	2.89179064
HTR3C	1.850394057	NA	NA
ALOX5	0.855502479	0.467755885	1.82895075
OGDHL	0.83318323	1.141132077	0.73013742
MATK	0.815029157	NA	NA
PIK3CG	1.103714386	0.73167938	1.50846726
PLCG2	0.871942447	0.249476603	3.49508706
PTGS1	0.673534891	0.461933218	1.45807849
IL17RB	0.8969865	0.467309219	1.91947101
GNG13	1.024981369	NA	NA
CAMP	2.260972819	NA	NA
ANKHD1	0.897739169	NA	NA
GIN1	1	NA	NA
SH2D7	0.658046427	0.328744382	2.00169634
BMX	1.360003183	0.360535132	3.77217936
HTR3E	0.848772333	NA	NA
AZGP1	1.029538915	0.515296922	1.99795277
TRPM5	0.599018856	0.314108919	1.90704186

668 **Supplementary Table 5**. Variability of the majority of 11q23.1 trans-eQTL targets is greater in Smillie *et*
669 *al.,* (2019) cluster 11 compared with Elmentaite *et al.,* (2021) cluster 18. Variability analysed within single
670 cells using Seurat *FindVariableGenes* (Hao et al., 2021). FC = Fold change of variability in Smillie *et al.,*
cluster 11 compared with Elmentaite *et al.,* (2021) cluster 18
671
672
673
674
675
676
677
678
679
680
681

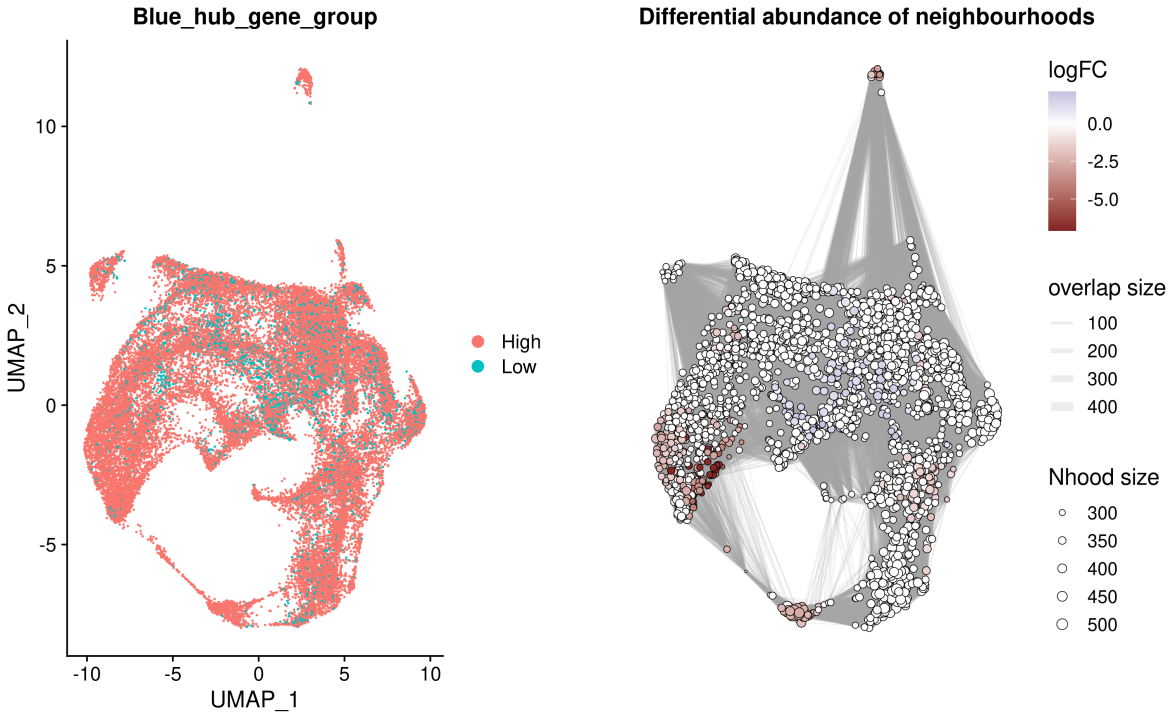

682 **Supplementary Figure 5.** UMAP of cells from each Blue module hub gene group (left) and the
683 differential abundance score of miloR-identified (Dann *et al.,* 2021) neighbourhoods (right).
684
685
686
687
688
689
690
691
692
693
694
695
696
697
698
699
700
701

References

Banerjee, A., Herring, C. A., Chen, B., Kim, H., Simmons, A. J., Southard-Smith, A. N., Allaman, M. M., White, J. R., Macedonia, M. C., Mckinley, E. T., Ramirez-Solano, M. A., Scoville, E. A., Liu, Q., Wilson, K. T., Coffey, R. J., Washington, M. K., Goettel, J. A., & Lau, K. S. (2020). Succinate Produced by Intestinal Microbes Promotes Specification of Tuft Cells to Suppress Ileal Inflammation. *Gastroenterology*, *159*(6). https://doi.org/10.1053/j.gastro.2020.08.029

Benjamini, Y., & Hochberg, Y. (1995). Controlling the false discovery rate: A practical and powerful approach to multiple testing. *Journal of the Royal Statistical Society*, *57*(1), 289–300.

Biancolella, M., Fortini, B. K., Tring, S., Plummer, S. J., Mendoza-Fandino, G. A., Hartiala, J., Hitchler, M. J., Yan, C., Schumacher, F. R., Conti, D. v., Edlund, C. K., Noushmehr, H., Coetzee, S. G., Bresalier, R. S., Ahnen, D. J., Barry, E. L., Berman, B. P., Rice, J. C., Coetzee, G. A., & Casey, G. (2014). Identification and characterization of functional risk variants for colorectal cancer mapping to chromosome 11q23.1. *Human Molecular Genetics*, *23*(8). https://doi.org/10.1093/hmg/ddt584

Blackmur, J. P., Vaughan-Shaw, P. G., Donnelly, K., Harris, B. T., Svinti, V., Ochocka-Fox, A.-M., Freile, P., Walker, M., Gurran, T., Reid, S., Semple, C. A., Din, F. V. N., Timofeeva, M., Dunlop, M. G., & Farrington, S. M. (2022). Gene Co-Expression Network Analysis Identifies Vitamin D-Associated Gene Modules in Adult Normal Rectal Epithelium Following Supplementation. *Frontiers in Genetics*, *12*. https://doi.org/10.3389/fgene.2021.783970

Butts, Carter. T. (2008). network: A package for managing relational data in R. *Journal of Statistical Software*, *24*(2).

Closa, A., Cordero, D., Sanz-Pamplona, R., Solé, X., Crous-Bou, M., Paré-Brunet, L., Berenguer, A., Guino, E., Lopez-Doriga, A., Guardiola, J., Biondo, S., Salazar, R., & Moreno, V. (2014). Identification of candidate susceptibility genes for colorectal cancer through eQTL analysis. *Carcinogenesis*, *35*(9). https://doi.org/10.1093/carcin/bgu092

Danecek, P., Bonfield, J. K., Liddle, J., Marshall, J., Ohan, V., Pollard, M. O., Whitwham, A., Keane, T., McCarthy, S. A., Davies, R. M., & Li, H. (2021). Twelve years of SAMtools and BCFtools. *GigaScience*, *10*(2). https://doi.org/10.1093/gigascience/giab008

Dann, E., Henderson, N. C., Teichmann, S. A., Morgan, M. D., & Marioni, J. C. (2021). Differential abundance testing on single-cell data using k-nearest neighbor graphs. *Nature Biotechnology*. https://doi.org/10.1038/s41587-021-01033-z

DelGiorno, K. E., Chung, C.-Y., Vavinskaya, V., Maurer, H. C., Novak, S. W., Lytle, N. K., Ma, Z., Giraddi, R. R., Wang, D., Fang, L., Naeem, R. F., Andrade, L. R., Ali, W. H., Tseng, H., Tsui, C., Gubbala, V. B., Ridinger-Saison, M., Ohmoto, M., Erikson, G. A., … Wahl, G. M. (2020). Tuft Cells Inhibit Pancreatic Tumorigenesis in Mice by Producing Prostaglandin D2. *Gastroenterology*, *159*(5). https://doi.org/10.1053/j.gastro.2020.07.037

Elmentaite, R., Kumasaka, N., Roberts, K., Fleming, A., Dann, E., King, H. W., Kleshchevnikov, V., Dabrowska, M., Pritchard, S., Bolt, L., Vieira, S. F., Mamanova, L., Huang, N., Perrone, F., Goh Kai'En, I., Lisgo, S. N., Katan, M., Leonard, S., Oliver, T. R. W., … Teichmann, S. A. (2021). Cells of the human intestinal tract mapped across space and time. *Nature*, *597*(7875). https://doi.org/10.1038/s41586-021-03852-1

Finak, G., McDavid, A., Yajima, M., Deng, J., Gersuk, V., Shalek, A. K., Slichter, C. K., Miller, H. W., McElrath, M. J., Prlic, M., Linsley, P. S., & Gottardo, R. (2015). MAST: a flexible statistical framework for assessing transcriptional changes and characterizing heterogeneity in single-cell RNA sequencing data. *Genome Biology*, *16*(1), 278. https://doi.org/10.1186/s13059-015-0844-5

Garrison, E., & Marth, G. (2012). *Haplotype-based variant detection from short-read sequencing*.

Gerbe, F., Sidot, E., Smyth, D. J., Ohmoto, M., Matsumoto, I., Dardalhon, V., Cesses, P., Garnier, L., Pouzolles, M., Brulin, B., Bruschi, M., Harcus, Y., Zimmermann, V. S., Taylor, N., Maizels, R. M., & Jay, P. (2016). Intestinal epithelial tuft cells initiate type 2 mucosal immunity to helminth parasites. *Nature*, *529*(7585). https://doi.org/10.1038/nature16527

752 Gerbe, F., van Es, J. H., Makrini, L., Brulin, B., Mellitzer, G., Robine, S., Romagnolo, B., Shroyer, N.
753 F., Bourgaux, J.-F., Pignodel, C., Clevers, H., & Jay, P. (2011). Distinct ATOH1 and Neurog3
754 requirements define tuft cells as a new secretory cell type in the intestinal epithelium. *Journal of*
755 *Cell Biology*, *192*(5). https://doi.org/10.1083/jcb.201010127
756 Graff, R. E., Möller, S., Passarelli, M. N., Witte, J. S., Skytthe, A., Christensen, K., Tan, Q., Adami, H.-
757 O., Czene, K., Harris, J. R., Pukkala, E., Kaprio, J., Giovannucci, E. L., Mucci, L. A., &
758 Hjelmborg, J. B. (2017). Familial Risk and Heritability of Colorectal Cancer in the Nordic Twin
759 Study of Cancer. *Clinical Gastroenterology and Hepatology*, *15*(8), 1256–1264.
760 https://doi.org/10.1016/j.cgh.2016.12.041
761 Griffiths, J. A., Richard, A. C., Bach, K., Lun, A. T. L., & Marioni, J. C. (2018). Detection and removal
762 of barcode swapping in single-cell RNA-seq data. *Nature Communications*, *9*(1), 2667.
763 https://doi.org/10.1038/s41467-018-05083-x
764 Haber, A. L., Biton, M., Rogel, N., Herbst, R. H., Shekhar, K., Smillie, C., Burgin, G., Delorey, T. M.,
765 Howitt, M. R., Katz, Y., Tirosh, I., Beyaz, S., Dionne, D., Zhang, M., Raychowdhury, R., Garrett,
766 W. S., Rozenblatt-Rosen, O., Shi, H. N., Yilmaz, O., … Regev, A. (2017). A single-cell survey of
767 the small intestinal epithelium. *Nature*, *551*(7680). https://doi.org/10.1038/nature24489
768 Hao, Y., Hao, S., Andersen-Nissen, E., Mauck, W. M., Zheng, S., Butler, A., Lee, M. J., Wilk, A. J.,
769 Darby, C., Zager, M., Hoffman, P., Stoeckius, M., Papalexi, E., Mimitou, E. P., Jain, J.,
770 Srivastava, A., Stuart, T., Fleming, L. M., Yeung, B., … Satija, R. (2021). Integrated analysis of
771 multimodal single-cell data. *Cell*, *184*(13). https://doi.org/10.1016/j.cell.2021.04.048
772 Hoffman, M. T., Kemp, S. B., Salas-Escabillas, D. J., Zhang, Y., Steele, N. G., The, S., Long, D.,
773 Benitz, S., Yan, W., Margolskee, R. F., Bednar, F., Pasca di Magliano, M., Wen, H.-J., &
774 Crawford, H. C. (2021). The Gustatory Sensory G-Protein GNAT3 Suppresses Pancreatic
775 Cancer Progression in Mice. *Cellular and Molecular Gastroenterology and Hepatology*, *11*(2).
776 https://doi.org/10.1016/j.jcmgh.2020.08.011
777 Hulur, I., Gamazon, E. R., Skol, A. D., Xicola, R. M., Llor, X., Onel, K., Ellis, N. A., & Kupfer, S. S.
778 (2015). Enrichment of inflammatory bowel disease and colorectal cancer risk variants in colon
779 expression quantitative trait loci. *BMC Genomics*, *16*(1). https://doi.org/10.1186/s12864-015-
780 1292-z
781 Huyghe, J. R., Bien, S. A., Harrison, T. A., Kang, H. M., Chen, S., Schmit, S. L., Conti, D. v., Qu, C.,
782 Jeon, J., Edlund, C. K., Greenside, P., Wainberg, M., Schumacher, F. R., Smith, J. D., Levine,
783 D. M., Nelson, S. C., Sinnott-Armstrong, N. A., Albanes, D., Alonso, M. H., … Peters, U. (2019).
784 Discovery of common and rare genetic risk variants for colorectal cancer. *Nature Genetics*,
785 *51*(1). https://doi.org/10.1038/s41588-018-0286-6
786 Jasperson, K. W., Tuohy, T. M., Neklason, D. W., & Burt, R. W. (2010). Hereditary and Familial Colon
787 Cancer. *Gastroenterology*, *138*(6). https://doi.org/10.1053/j.gastro.2010.01.054
788 Kaske, S., Krasteva, G., König, P., Kummer, W., Hofmann, T., Gudermann, T., & Chubanov, V.
789 (2007). TRPM5, a taste-signaling transient receptor potential ion-channel, is a ubiquitous
790 signaling component in chemosensory cells. *BMC Neuroscience*, *8*(1).
791 https://doi.org/10.1186/1471-2202-8-49
792 Kjærgaard, S., Jensen, T. S. R., Feddersen, U. R., Bindslev, N., Grunddal, K. v., Poulsen, S. S.,
793 Rasmussen, H. B., Budtz-Jørgensen, E., & Berner-Hansen, M. (2021). Decreased number of
794 colonic tuft cells in quiescent ulcerative colitis patients. *European Journal of Gastroenterology &*
795 *Hepatology*, *33*(6). https://doi.org/10.1097/MEG.0000000000001959
796 Korotkevich, G., Sukhov, V., Budin, N., Shpak, B., Artyomov, M. N., & Sergushichev, A. (2021). Fast
797 gene set enrichment analysis. *BioRxiv*.
798 Langfelder, P., & Horvath, S. (2008). WGCNA: an R package for weighted correlation network
799 analysis. *BMC Bioinformatics*, *9*(1). https://doi.org/10.1186/1471-2105-9-559
800 Law, P. J., Timofeeva, M., Fernandez-Rozadilla, C., Broderick, P., Studd, J., Fernandez-Tajes, J.,
801 Farrington, S., Svinti, V., Palles, C., Orlando, G., Sud, A., Holroyd, A., Penegar, S.,

802 Theodoratou, E., Vaughan-Shaw, P., Campbell, H., Zgaga, L., Hayward, C., Campbell, A., …
803 Dunlop, M. G. (2019). Association analyses identify 31 new risk loci for colorectal cancer
804 susceptibility. *Nature Communications*, *10*(1). https://doi.org/10.1038/s41467-019-09775-w
805 Liu, F., Zhang, Y., Zhang, L., Li, Z., Fang, Q., Gao, R., & Zhang, Z. (2019). Systematic comparative
806 analysis of single-nucleotide variant detection methods from single-cell RNA sequencing data.
807 *Genome Biology*, *20*(1), 242. https://doi.org/10.1186/s13059-019-1863-4
808 Loo, L. W. M., Lemire, M., & le Marchand, L. (2017). In silico pathway analysis and tissue specific cis-
809 eQTL for colorectal cancer GWAS risk variants. *BMC Genomics*, *18*(1).
810 https://doi.org/10.1186/s12864-017-3750-2
811 Luo, Y., Coskun, V., Liang, A., Yu, J., Cheng, L., Ge, W., Shi, Z., Zhang, K., Li, C., Cui, Y., Lin, H.,
812 Luo, D., Wang, J., Lin, C., Dai, Z., Zhu, H., Zhang, J., Liu, J., Liu, H., … Li, S. (2015). Single-Cell
813 Transcriptome Analyses Reveal Signals to Activate Dormant Neural Stem Cells. *Cell*, *161*(5).
814 https://doi.org/10.1016/j.cell.2015.04.001
815 McCarthy, D. J., Chen, Y., & Smyth, G. K. (2012). Differential expression analysis of multifactor RNA-
816 Seq experiments with respect to biological variation. *Nucleic Acids Research*, *40*(10).
817 https://doi.org/10.1093/nar/gks042
818 McGinnis, C. S., Murrow, L. M., & Gartner, Z. J. (2019). DoubletFinder: Doublet Detection in Single-
819 Cell RNA Sequencing Data Using Artificial Nearest Neighbors. *Cell Systems*, *8*(4).
820 https://doi.org/10.1016/j.cels.2019.03.003
821 Michaelson, J. J., Loguercio, S., & Beyer, A. (2009). Detection and interpretation of expression
822 quantitative trait loci (eQTL). *Methods*, *48*(3). https://doi.org/10.1016/j.ymeth.2009.03.004
823 Middelhoff, M., Westphalen, C. B., Hayakawa, Y., Yan, K. S., Gershon, M. D., Wang, T. C., & Quante,
824 M. (2017). Dclk1-expressing tuft cells: critical modulators of the intestinal niche? *American*
825 *Journal of Physiology-Gastrointestinal and Liver Physiology*, *313*(4).
826 https://doi.org/10.1152/ajpgi.00073.2017
827 Rawla, P., Sunkara, T., & Barsouk, A. (2019). Epidemiology of colorectal cancer: incidence, mortality,
828 survival, and risk factors. *Gastroenterology Review*, *14*(2).
829 https://doi.org/10.5114/pg.2018.81072
830 Richards, A. L., Jones, L., Moskvina, V., Kirov, G., Gejman, P. v, Levinson, D. F., Sanders, A. R.,
831 Purcell, S., Visscher, P. M., Craddock, N., Owen, M. J., Holmans, P., & O'Donovan, M. C.
832 (2012). Schizophrenia susceptibility alleles are enriched for alleles that affect gene expression in
833 adult human brain. *Molecular Psychiatry*, *17*(2). https://doi.org/10.1038/mp.2011.11
834 Ritchie, M. E., Phipson, B., Wu, D., Hu, Y., Law, C. W., Shi, W., & Smyth, G. K. (2015). limma powers
835 differential expression analyses for RNA-sequencing and microarray studies. *Nucleic Acids*
836 *Research*, *43*(7). https://doi.org/10.1093/nar/gkv007
837 Smillie, C. (2015). *Functional characterisation of the 11q23.1 colorectal cancer risk locus*, PhD thesis,
838 The University of Edinburgh, Edinburgh
839 Smillie, C. S., Biton, M., Ordovas-Montanes, J., Sullivan, K. M., Burgin, G., Graham, D. B., Herbst, R.
840 H., Rogel, N., Slyper, M., Waldman, J., Sud, M., Andrews, E., Velonias, G., Haber, A. L.,
841 Jagadeesh, K., Vickovic, S., Yao, J., Stevens, C., Dionne, D., … Regev, A. (2019). Intra- and
842 Inter-cellular Rewiring of the Human Colon during Ulcerative Colitis. *Cell*, *178*(3).
843 https://doi.org/10.1016/j.cell.2019.06.029
844 Stranger, B. E., Nica, A. C., Forrest, M. S., Dimas, A., Bird, C. P., Beazley, C., Ingle, C. E., Dunning,
845 M., Flicek, P., Koller, D., Montgomery, S., Tavaré, S., Deloukas, P., & Dermitzakis, E. T. (2007).
846 Population genomics of human gene expression. *Nature Genetics*, *39*(10).
847 https://doi.org/10.1038/ng2142
848 Sud, A., Kinnersley, B., & Houlston, R. S. (2017). Genome-wide association studies of cancer: current
849 insights and future perspectives. *Nature Reviews Cancer*, *17*(11).
850 https://doi.org/10.1038/nrc.2017.82

Tenesa, A., Farrington, S. M., Prendergast, J. G. D., Porteous, M. E., Walker, M., Haq, N., Barnetson, R. A., Theodoratou, E., Cetnarskyj, R., Cartwright, N., Semple, C., Clark, A. J., Reid, F. J. L., Smith, L. A., Kavoussanakis, K., Koessler, T., Pharoah, P. D. P., Buch, S., Schafmayer, C., … Dunlop, M. G. (2008). Genome-wide association scan identifies a colorectal cancer susceptibility locus on 11q23 and replicates risk loci at 8q24 and 18q21. *Nature Genetics*, *40*(5). https://doi.org/10.1038/ng.133

Vaughan-Shaw, Peter. G., Timofeeva, M., Ooi, L., Svinti, V., Grimes, G., Smillie, C., Blackmur, J. P., Donnelly, K., Theodoratou, E., Campbell, H., Zgaga, L., Din, F. V. N., Farrington, S. M., & Dunlop, M. G. (2021). Differential genetic influences over colorectal cancer risk and gene expression in large bowel mucosa. *International Journal of Cancer*, *149*(5). https://doi.org/10.1002/ijc.33616

Wei, T., & Simko, V. (2017). *"Corrplot": Visualization of a Correlation Matrix (Version 0.84).*

Wickham, H. (2009). *ggplot2: Elegant graphics for data analysis*. Springer-Verlag.

Wu, C.-L., Dicks, A., Steward, N., Tang, R., Katz, D. B., Choi, Y.-R., & Guilak, F. (2021). Single cell transcriptomic analysis of human pluripotent stem cell chondrogenesis. *Nature Communications*, *12*(1). https://doi.org/10.1038/s41467-020-20598-y

Yamaga, Y., Fukuda, A., Nakanishi, Y., Goto, N., Matsumoto, Y., Yoshioka, T., Maruno, T., Chiba, T., & Seno, H. (2018). Gene expression profile of Dclk1+ cells in intestinal tumors. *Digestive and Liver Disease*, *50*(12). https://doi.org/10.1016/j.dld.2018.06.011

Yi, J., Bergstrom, K., Fu, J., Shan, X., McDaniel, J. M., McGee, S., Qu, D., Houchen, C. W., Liu, X., & Xia, L. (2019). Dclk1 in tuft cells promotes inflammation-driven epithelial restitution and mitigates chronic colitis. *Cell Death & Differentiation*, *26*(9). https://doi.org/10.1038/s41418-018-0237-x

Zheng, G. X. Y., Terry, J. M., Belgrader, P., Ryvkin, P., Bent, Z. W., Wilson, R., Ziraldo, S. B., Wheeler, T. D., McDermott, G. P., Zhu, J., Gregory, M. T., Shuga, J., Montesclaros, L., Underwood, J. G., Masquelier, D. A., Nishimura, S. Y., Schnall-Levin, M., Wyatt, P. W., Hindson, C. M., … Bielas, J. H. (2017). Massively parallel digital transcriptional profiling of single cells. *Nature Communications*, *8*(1). https://doi.org/10.1038/ncomms14049

Acknowledgements

Funding: This work was supported by Cancer Research UK (CRUK) PhD studentship at the Edinburgh CRUK Cancer Research Centre (Bradley T. Harris / Susan M. Farrington) and CRUK programme grant DRCPGM\100012 (Malcolm G. Dunlop / Susan M. Farrington). James P. Blackmur was supported by an ECAT-linked CRUK ECRC Clinical training award (C157/A23218). Peter Vaughan-Shaw was supported by a NES SCREDS clinical lectureship, MRC Clinical Research Training Fellowship (MR/M004007/1), a Research Fellowship from the Harold Bridges bequest and by the Melville Trust for the Care and Cure of Cancer. **Competing Interests:** The authors declare no competing interests. **Data availability:** All data used in this study has been referenced within the Materials and Methods. **Open Access:** For the purpose of open access, the author has applied a Creative Commons Attribution (CC BY) licence to any Author Accepted Manuscript version arising from this submission.